An analysis of offshore wind farm SCADA measurements to identify key parameters influencing the magnitude of wake effects

Niko Mittelmeier[1], Julian Allin[1], Tomas Blodau[1], Davide Trabucchi[2], Gerald Steinfeld[2], Andreas Rott[2] and Martin Kühn[2]

[1] Senvion GmbH, Überseering 10, 22297 Hamburg, Germany
[2] ForWind – University of Oldenburg, Institute of Physics, Küpkersweg 70, 26129 Oldenburg

Correspondence to: Niko Mittelmeier (niko.mittelmeier@senvion.com)

Abstract. For offshore wind farms wake effects are among the largest sources for losses in energy production. At the same time wake modelling is still associated with very high uncertainties. Therefore current research focusses on improving wake model predictions. It is known that atmospheric conditions, especially atmospheric stability, crucially influence the magnitude of those wake effects. The classification of atmospheric stability is usually based on measurements from met masts, buoys or LiDARs (Light Detection and Ranging). In offshore conditions these measurements are expensive and scarce. However, every wind farm permanently produces SCADA (Supervisory Control and Data Acquisition) measurements. The objective of this study is to establish a classification for the magnitude of wake effects based on SCADA data. This delivers a basis to fit engineering wake models better to the ambient conditions in an offshore wind farm. ~~Atmospheric conditions have a clear influence on wake effects. Stability classification is usually based on wind speed, turbulence intensity, shear and temperature gradients measured partly at met masts, buoys or LiDARs. The objective of this paper is to find a classification for stability based on wind turbine Supervisory Control and Data Acquisition (SCADA) measurements in order to fit engineering wake models better to the current ambient conditions. Two offshore wind farms with met masts~~The method is established with data from two offshore wind farms, which have a met mast nearby each. A correlation is established between the stability classification from the met mast and signals within the SCADA data from the wind farm.~~ have been used to establish a correlation between met mast stability classification and new aggregated artificial signals.~~ The significance of these new signals on power production is demonstrated with data~~for~~ from two wind farms with met mast~~s~~ and ~~measurements from a~~ long range LiDAR measurements. Additionally the method~~and~~ is validated ~~against~~ with data from ~~one further~~another wind farm without ~~a~~ met mast. The proposed signal consists of a good correlation between the standard deviation of active power divided by the average power of wind turbines in free flow, with the ambient turbulence intensity TI, ~~We found a good correlation between the standard deviation of active power divided by the average power of wind turbines in free flow with the ambient turbulence intensity~~ when the wind turbines were operating in partial load. It allows to distinguish between conditions with different magnitude of wake effects. The proposed signal is very sensitive to increased turbulence ~~due to~~induced by neighbouring turbines and wind farms, even at a distance of more than 38 rotor diameters. ~~away. It allows to distinguish between conditions with different magnitude of wake effects.~~

1 Introduction

Wake effects are one of the largest sources of losses in offshore energy yield assessment. This makes wake modelling very important and much research is ongoing to improve wake model predictions. In the latest offshore CREYAP ~~-~~benchmark exercise (Comparative Resource and Energy Yield Assessment Procedure) wake modelling was found to be the prediction with the highest variation among the participants (Mortensen et al., 2015).

In order to be able to use a wake model for validating the performance of an operating offshore wind farm (Mittelmeier et al., 2017)~~(Mittelmeier et al., 2016)~~ prediction uncertainties need to be reduced. Hansen et al. (2012) studied wake effects at the offshore wind farm Horns Rev in different atmospheric conditions and revealed an influence on the wake magnitude. They also compared turbulence intensities for different stability classes as a function of the wind speed. Below 7 m/s a clear increase in turbulence intensities can be noticed. Above 7 m/s neutral-unstable conditions are distinguishable from more stable conditions with a constant threshold up to nominal wind speed. Dörenkämper et al. (2014) draw a link from stability via shear to turbulence intensity motivated by the studies of Tambke et al. (2005) and showed its impact on wake effects. Sanz Rodrigo et al. (2015) compared different stability classification methodologies with data from FINO 1 and presented the behavior of shear and turbulence intensity for the proposed atmospheric stability classes. The authors concluded, that in this particular case TI correlates well for stable cases but at near neutral and unstable cases, shear is supposed to enable better distinction between their proposed nine classes. ~~-~~Atmospheric stability as well as turbulence intensity ha~~s~~ve been identified as being ~~one~~ main drivers for the variation in power production under waked conditions (Dörenkämper et al., 2012~~,~~; Westerhellweg et al., 2014~~;~~, Iungo and Porté-Agel, 2014)~~.~~, ~~and~~ Therefore state of the art engineering wake models for industrial application like Fuga or FarmFlow are able to take stability effects into account (Özdemir et al., 2013, Ott and Nielsen, 2014).

Stability classification is based on measurements from met masts, buoys or is assisted by remote sensing devices such as Light Detection and Ranging (LiDAR) or Sound Detection and Ranging (SoDAR). For offshore use, these devices are very expensive and therefore often not permanently available. In several studies, LIDAR's have been used to assess the wind speed recovery behind the turbine and wake models have been tuned to match the measured wind speed (Beck et al., 2014, More and Gallacher, 2014).

The purpose of this paper is to investigate wind farm operational data and establish methods of identifying correlations between SCADA statistics and wind turbine wake behaviour caused by different atmospheric conditions.

2 Wind farms and measurements

For this investigation, we select three offshore wind farms, i.e. alpha ventus, Nordsee Ost and Ormonde. The first two wind farms have a well-equipped met mast and provide high quality measurements of hub height wind speed, wind direction, shear and turbulence intensity as well as water temperature.

Feldfunktion geändert

Kommentar [RC1-1]: - A direct correlation is expected between the turbulence intensity and the atmospheric stability. Though, for a fixed stability condition, turbulence intensity can have big scatter and particularly at low wind speeds. Reference to the works from Dorenkampfer et al. (2012 and 2015) are used to justify this strong simplification but these references are a PhD thesis and a proceeding from a national conference. I would suggest to make references to publications in peer-review journals and to develop the arguments that give the possibility to reduce the stability effect to a turbulence intensity effect, and particularly at low Wind speeds.

Formatiert: Schwedisch (Schweden)

Formatiert: Schwedisch (Schweden)

Formatiert: Schwedisch (Schweden)

Formatiert: Englisch (USA)

Feldfunktion geändert

2.1 alpha ventus

The wind farm alpha ventus (AV) is located about 45 km north of the island of Borkum in the North Sea. It consists of twelve turbines of the 5 MW class with a rotor diameter of 126 m and has been commissioned in April 2010. The six northern turbines (AV1 – AV6) have been manufactured by Senvion. The six turbines in the southern part of the wind farm ~~(produced~~ are manufactured by Adwen~~) are~~ and not considered in ~~our~~ this analysis. The FINO1 research met mast is located only 3.2 D (rotor diameters) west of turbine AV4.

> **Kommentar [RC2-2]:** Page 2, line 12 ‘rotordiameter’ is missing a space.

The layout of the northern part of alpha ventus (See Fig. 1) allows for investigating the wake behaviour in single and double wake conditions for westerly wind directions. ~~No d~~Data ~~after the period~~was used from 3/2011 to 1/2015. ~~is used~~After 1/2015 no data was used, because the installation of the Trianel wind farm in the west is ~~supposed~~ suspected to have changed the environmental conditions of alpha ventus by adding extra turbulence to the inflow.

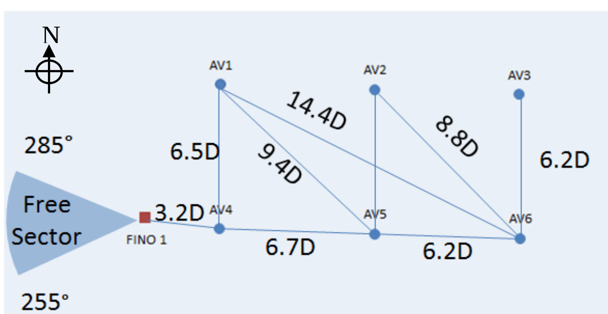

Figure 1: Scematic Layout of the ~~N~~northern part of alpha ventus wind farm (circles) and FINO1 met mast (red square) ~~layout~~ with free flow sector and distance in rotor diameters

2.2 Nordsee Ost

The wind farm Nordsee Ost (NO) is located about 35 km north-west of the island of Helgoland in the North Sea. The 48 Senvion turbines have a rated power of 6 MW each and a rotor diameter of 126 m. The met mast is located in the south-western corner of the wind farm (See Fig. 2). In the south, the neighbouring wind farm Meerwind Ost/Süd reduces the sector of free flow for the met mast as well as the possibilities to study multiple wakes higher than triple wake condition without disturbing effects from Meerwind.

The wind farm Nordsee Ost has been fully commissioned in 2015. ~~So far not enough data~~Data for this analysis is selected from ~~(~~11/2015 – 11/2016.~~) has been collected to investigate the full wake behaviour based on SCADA data. For this reason, a~~ A correlation analysis (described in ~~Section~~Sect. 3.2) is performed and the data from ~~the~~ a ~~ClusterDesign~~ long range LiDAR ~~measurement campaign~~ is analysed. This LiDAR measurement campaign took place within the European Research Project “ClusterDesign”.

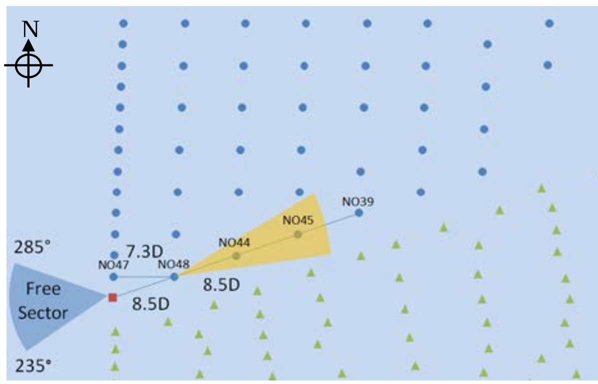

Figure 2: Nordsee Ost wind farm (blue ~~cycles~~circles) with neighbouring wind farm Meerwind Süd (green triangles) ~~and~~ ,met mast (red square) and distance in rotor diameter (D). Orange area indicates the Plan Position Indicator (PPI) scan from the Windcube 200S, mounted on the helicopter platform of NO48. (Described in Sect. 2.5)

Kommentar [RC2-3]: Page 3, fig 2 caption 'cycles' should be 'circles'.

2.3 Ormonde

The Ormonde wind farm consists of 30 Senvion turbines with a rated power of 5 MW each and a rotor diameter of 126 m. The wind farm is located in the Irish Sea 10 km west of the Isle of Walney. The selected data is from 1/2012 – 1/2014. During this period, neighbouring wind farms were operational. Located ~~I~~in the south west~~, there~~ are ~~is~~ Walney~~-~~ 1 (51 x SWT-3.6-107 Siemens) and Walney 2 (51 x SWT-3.6-120 Siemens), located in the south there is West of Duddon Sands (SWT-3.6-120 Siemens, fully commissioned 30.10.2014) and in the south east there is Barrow (V90 3.0MW Vestas).

The farm layout displayed in Fig. 3 is structured in a regular array which allows for comparing several multiple-wake situations. The inner farm turbine distance for the investigated wake situation from south west is 6.3 D and from north west is 4.3 D.

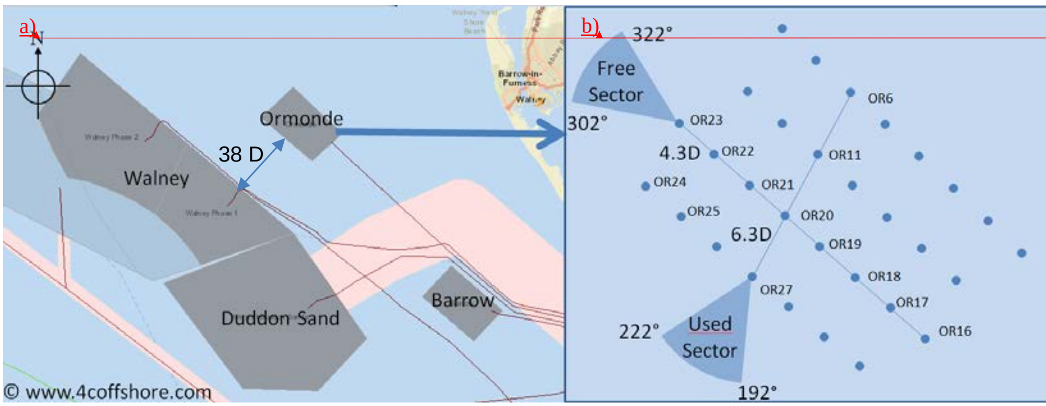

Figure 3: a) Ormonde and neighbouring wind farm~~s and its neighbours~~. ~~Two wind directions are selected for the analysis of wake effects at different turbulent classes.~~ b) Ormonde wind farm layout with distances in rotor diameters (D) and sectors selected for the analysis.

2.4 SCADA and meteorological data

The SCADA data from all wind farms and the meteorological data consist of 10-min statistics. Each turbine provides wind speed, wind direction, active power, yaw position, and pitch angle. The operational condition of the wind turbine which is used for the correlation with the met mast turbulence intensity is categorized by the minimum active power > 10kW, the maximum pitch angle < 3 ° and the standard deviation of the yaw position < 5 °. These filter criteria's ensure that no stand stills, curtailments or too large yaw activities are included in the data. Furthermore any succeeding 10-min measurement period after a turbine restart is deleted to give the flow enough time to develop. SCADA data are also deleted if the waked turbine produces more power than the free flow turbine. Implausible met mast data ~~is~~ are removed and wind directions ~~is~~ are corrected for bias by using the orientation of the maximum wake deficit. For the correlation, only sectors of free flow conditions ~~is~~ are used. Averages of 30-min water temperature are recorded by buoys at FINO1 and linearly interpolated into the SCADA data.

2.5 Long range LiDAR measurements

Within the "ClusterDesign" research project, funded by the European Union, a long-range LiDAR measurement campaign was realized. A Windcube 200S (WLS200S) LiDAR with scan head was placed on the helicopter platform of NO48 (See ~~Fig. 2~~Fig. 2) from 11/2015 – 5/2016. A differential GPS system composed by three antenna GNSS-Systems of type Trimble SPS855 / SPS555H ~~allowes~~allows for additional measurements of turbines~~`s~~ yaw and nacelle~~`s~~ pitch and roll angle. One LiDAR measurement cycle takes about 200~~-~~s. It ~~includs~~includes five ~~plan~~ Plan ~~position~~ Position ~~indicator~~ Indicator (PPI) scans followed by one ~~range~~ Range ~~height~~ Height ~~indicator~~ Indicator (RHI) scan. Both scans cover a sector of 30~~-~~° on the

Formatiert: Deutsch (Deutschland)

Formatiert: Deutsch (Deutschland)

Kommentar [RC2-4]: Page 4, lines 11 and 12 There are two instances where 'is' should be 'are'.

Kommentar [RC2-5]: Page 4, lines 17 and 18 There are two spelling errors: 'allowes' and 'includs'. Also the possessive is not necessary for 'turbine' and 'nacelle'.

horizontal and vertical plane respectively and are centred on the rotor axis. The scan trajectories have an angular resolution of 1~~-~~° and measure~~d~~ the wind speed component along the measuring direction every 25 m from 100 m to 2500 m. The LiDAR data is filtered excluding measurements with a poor signal intensity,~~ or~~ affected by hard targets~~, or~~and considered outliers.

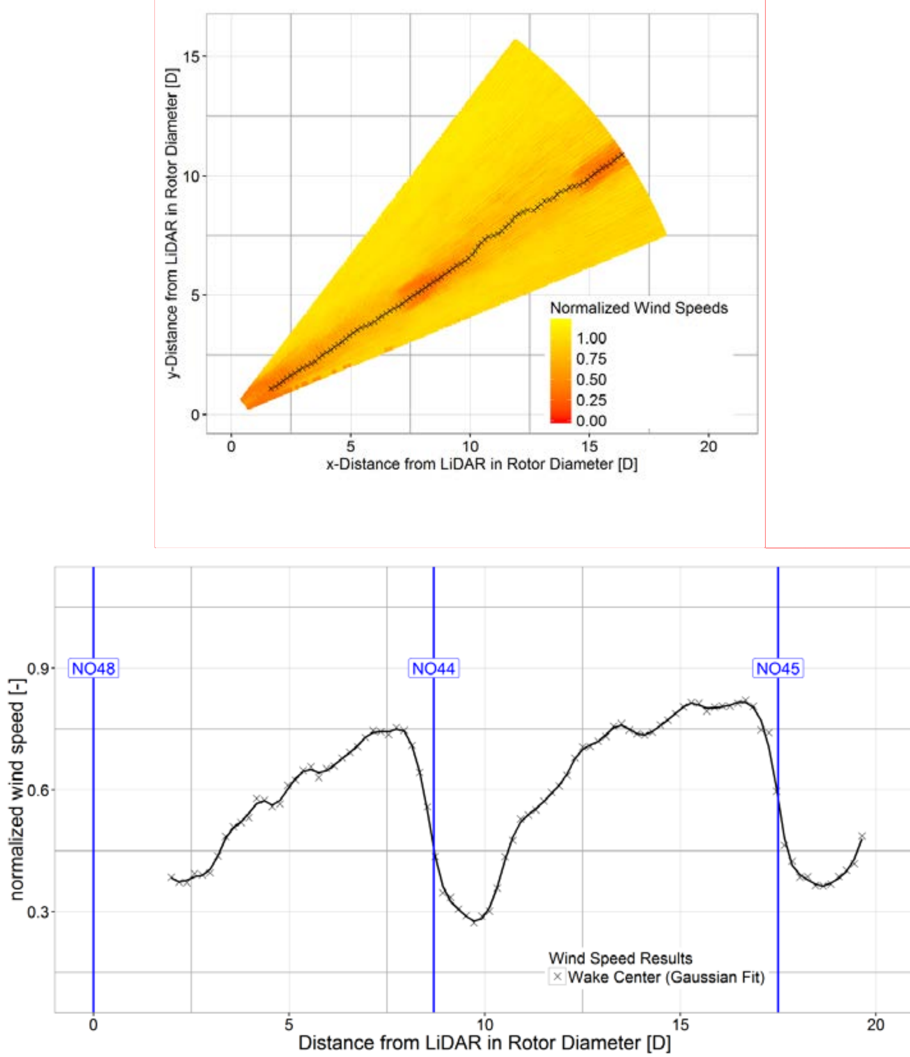

Figure 4: Upper-plot: Visualization of the horizontal plan position indicator (PPI) scans downstream of NO48. Wind speed is normalized with the inflow wind speed, measured at the met mast. The black crosses are the locations of the wind speed minima's derived from a Gaussian fitting for each measurement distance. Bottom-plot: Normalized wind speed as function of the distance in rotor diameters, extracted from the top-plot for the Gaussian fitted minima's (black crosses).

Kommentar [RC1-6]: - LiDAR measurements at Nord See wind farm NO : PPI planes are described as horizontal. LiDAR is located on the helicopter platform from the wind turbine NO48. One therefore guess that is corresponds to an altitude close to the hub height. Consequently, the laser beam should meet the wind turbine rotors NO44 and NO45, leading to unusable data in the vicinity of both rotors. On the other hand, on Figure 4, the visualizations of the velocity field, as well as the normalized velocity evolution versus the downwind distance do not present any unresolved areas close to the rotors. The velocity induction through the rotor is presented and discussed. Please explain how these data were reconstructed close to the rotors.

The horizontal 10-min average wind speed is calculated on a well-defined grid under the assumption of a negligible vertical component of the wind. The average of the wind component measured by the LiDAR during the considered time interval is included in the region of interest of the addressed grid point. The average 10-min wind direction is provided by the met mast. When the latter measurement is not available, the turbine yaw provided by the differential GPS system is used to estimate the wind direction. A detailed description of the LiDAR data pre-processing can be found in Schneemann et al. (2016).

For the assessment in this paper we are using averages of 10-min periods of horizontal wind speed data evaluated from PPI scans of the wake behind NO48 (See Fig.2). A multiple wake situation can be observed at a wind direction of ~~236~~237.5 °, when NO45 is in the wake of NO44 and NO48. In Fig. 4 (top) an example for a PPI scan at hub height with averages of 10-min periods of the horizontal wind speed data is displayed. Hard targets like blades and nacelle prevent reasonable wind speed measurement. Wind speeds at these blind regions and between the beam directions are linearly interpolated. The distance from turbine NO48 is normalised by its rotor diameter and the wind speeds are normalized with the corresponding wind speed measured at the met mast. The different colours represent the wind speed relative to the wind speed at the given met mast location. The black crosses display the locations of the estimated wind speed minima for each measured distance equal or greater than 2 D. These minima are supposed to represent the centre of the wake. They are derived at each downstream cross-~~section~~section with a Gaussian smoothing (Hamilton, 2015) applied to the LiDAR data before fitting a double-Gaussian-type velocity deficit at the near wake (≤2.5 D~~2 D – 5 D~~) and a single-Gaussian-type in the far wake. This distinction prevents an overestimation of the deficit in the near wake where the nacelle still has an influence on the flow shape (Keane et al., 2016). The Gaussian minima (black crosses) do not follow a straight line for the entire scan. This should not be interpreted as meandering as we are looking at averages of 10-~~-~~min periods.

The lower graph of Fig. 4 shows the resulting, normalized wind speeds over the normalized distance from NO48. The black line with the corresponding black crosses refers to the fitted values of the Gaussian fits.

3 ~~Data analysis~~Method

Following the objective to propose a signal based on SCADA data that enables to identify the magnitude of wake effect, we first establish stability classification based on Monin-Obukhov surface-layer theory (Monin and Obukhov, 1954) and met mast turbulence intensity. Both approaches can be found in many publications and their influence on the magnitude of wake effects is reported. Secondly, SCADA signals which are effected by turbulence intensity are proposed and the ability of these signals to classify low, medium and high wake effects is analysed.

Formatiert: Standard, Tabstopps: Nicht an 7.91 cm

3.1. ~~Turbulence, stability and its impact on power production~~Stability and turbulence intensity classification

For the determination of atmospheric stability we follow the approach suggested by ~~(~~Ott and Nielsen~~,~~ (2014). Their iterative method is implemented in the software AMOK and derives the inverse Monin-Obukhov-Length $1/L$ from air temperature and wind speed measured at z $[m]$ and water surface temperature. Many different thresholds for stability classification have been published and breakdowns from three to nine different classes can be found in the literature (Archer et al., 2016~~)~~; ~~(~~Sanz Rodrigo et al., 2015). Dörenkämper (2015) and Rajewski et al. (2013) have suggested a classification into unstable, neutral and stable classes (Table 1) based on turbulence intensity (TI) and the dimensionless Monin-Obukhov-Length~~A stability classification according to the Richardson number expects wind speed and temperature measurements in 10 m and 30 m height. As both met masts fail to fulfil this requirement and as the available temperature measurements have a too large uncertainty to provide reliable stability estimates via the bulk Richardson approach (Saint-Drenan et al., 2009), the simplified classification using turbulence intensity at hub height as proposed by Dörenkämper et al. (2012, 2015) is used for this investigation.~~

~~SCADA and LiDAR data is divided into three subsets based on~~ $\zeta = \frac{z}{L}$. ~~the turbulence intensity from the met mast. Dörenkämper (2015) has suggested a classification into unstable, neutral and stable classes (Table 1). The power production for the different subsets, normalised by free flow power production, is compared for single wake and double wake conditions with data from alpha ventus and FINO1. This kind of analysis reveals the impact only at turbine positions but the wind speed behaviour in-between turbines is not covered. Therefore at Nordsee Ost, wind speed recovery in single, double and triple wake situations measured by the LiDAR is analysed.~~

~~To determine the influence of turbulence and stability on wake effects all available PPIs are analysed and the results of the Gaussian fitted minima's are divided into the same subsets as described in Table 1 based on the turbulence intensity measured at hub height with the met mast.~~

Table 1: Definition of stratification with turbulence intensity and the dimensionless Monin-Obukhov-Length ζ ~~by met mast turbulence intensity at hub height at alpha ventus and Nordsee Ost~~

Classification	~~Turbulence Intensity (TI)~~(Dörenkämper, 2015)	(Rajewski et al., 2013)
Unstable	TI > 6 %	$\zeta < -0.05$
Neutral	~~6~~ 4 % ~~≥~~ ≤ TI ~~≥~~ ≤ ~~4~~ 6 %	$-0.05 \leq \zeta \leq 0.05$
Stable	~~4 % >~~ TI < 4%	$\zeta > 0.05$

Both classifications and their impact on wake effects are compared with FINO1 data in Sect. 4.1 and alpha ventus data in Sect. 4.2.~~The power production for the different subsets, normalised by free flow power production, is compared for single wake and double wake conditions with data from alpha ventus and FINO1. This kind of analysis reveals the impact only at turbine positions but the wind speed behaviour in between turbines is not covered. Therefore at Nordsee Ost, wind speed recovery in single, double and triple wake situations measured by the LiDAR is analysed.~~

Kommentar [RC2-7]: Page 6, Sect. 3.1 It is surprising that a study specifically considering stability effects is relying on a simplified classification technique. This introduces a considerable amount of unnecessary uncertainty as an independent variable (i.e. the stability) is not directly measured.

Formatiert: Hervorheben

Feldfunktion geändert

Feldfunktion geändert

Kommentar [RC2-8]: Page 7, table 1 More discussion for the boundary values for TI is needed. How exactly were these values assigned to unstable, neutral, and stable?

Formatierte Tabelle

Formatiert: Standard

~~To determine the influence of turbulence and stability on wake effects all available PPIs are analysed and the results of the Gaussian fitted minima's are divided into the same subsets as described in Table 1 based on the turbulence intensity measured at hub height with the met mast.~~

Formatiert: Standard

3.2 Correlation analysis

At wind farms with no met mast we have to rely on other signals to describe the differences in power production under different atmospheric conditions. To find the best substitute for a met mast measured turbulence intensity several SCADA signals that are affected by turbulence are correlated to the met mast turbulence intensity which is defined as

$$TI_{mast} = \frac{\sigma_{u_{mast}}}{\overline{u_{mast}}} \ . \qquad (1)$$

Analogous to Eq. 1 we define

$$TI_{WT} = \frac{\sigma_{u_{WT}}}{\overline{u_{WT}}} \qquad (2)$$

as the turbulence intensity measured with the wind speed anemometer on top of the nacelle with $\bar{u}$ being averages of 10-min periods of horizontal wind speed and its standard deviation σ_u. Göçmen and Giebel (2016) evaluated 1Hz data from Lillgrund and Horns Rev I and found good turbulence estimators by using a turbine derived "WindEstimate" from look-up tables. When only 10-min statistics are available the signals of interest are the standard deviation of the turbine power

$$PO_{std} = \sigma_P, \qquad (3)$$

and the normalisation of this signal with the average power $\bar{P}$. This leads to

$$PO_{TI} = \frac{\sigma_P}{\bar{P}}. \qquad (4)$$

Kommentar [RC2-9]: Page 7, eq 4 I suspect, but cannot verify, that the decent correlation between the two may be (in part) happenstance. Atmospheric turbulence intensity decreases with wind speed as a result of flow physics. The standard deviation of output power to power also decreases with wind speed but largely because the turbine controller plays an increasingly active role. The authors allude to this later in the paper but more discussion of why eq 4 might be a suitable proxy for eq 1 would be of interest.

~~All SCADA signals can be obtained under free flow conditions or in waked conditions.~~Turbulence intensity is dependent on wind speed (Türk and Emeis, 2010). Wake effects are most pronounced at partial load and in this range, shear and PO_{TI} are even more related to wind speed. The relationship between PO_{TI} and the wind speed can be approximated with a third order polynomial,

$$y = \beta_0 + \beta_1 u + \beta_2 u^2 + \beta_3 u^3 + \varepsilon \ . \qquad (5)$$

y is the predicted outcome of the model, β_i are constants and u the wind speed. ε is the residual being normal distributed. Adjusting PO_{TI} with this model

$$PO_{TI_{norm}}(u) = \frac{PO_{TI}}{\beta_0 + \beta_1 u + \beta_2 u^2 + \beta_3 u^3} \qquad (6)$$

enables to select constant thresholds. For the wind speed range in partial load, the polynomial is always greater than zero. (At AV4 the constants of the third order polynomial are $\beta_0 = 99.9, \ \beta_1 = -32.5, \ \beta_2 = 3.9$ and $\beta_3 = -0.16$. See Sect. 4.4)

3.3 ~~New c~~Classification ~~and validation~~of wake magnitude

In this Section, we describe the methodology to establish thresholds for sub-setting the measurements into weak, medium and strong wake effects. ~~The new artificial SCADA signal with the highest correlation to the met mast turbulence intensity is used to classify different stratifications.~~ The thresholds are estimated with a ~~two~~three-step approach. At first we select the normalized power (waked turbine, normalized by the power of a free flow turbine) for a small sector (10°) in the full wake for the relevant wind speed range (8 ± 1 m/s) (Fig 5a). Secondly we eliminate the dependency on wind direction by subtracting from the normalized Power P_n its mean value of each wind direction bin (binwidth = 2°) and obtain P_{nn} (See Fig. 5b).

~~Fi~~

~~Fig~~

~~Fig~~

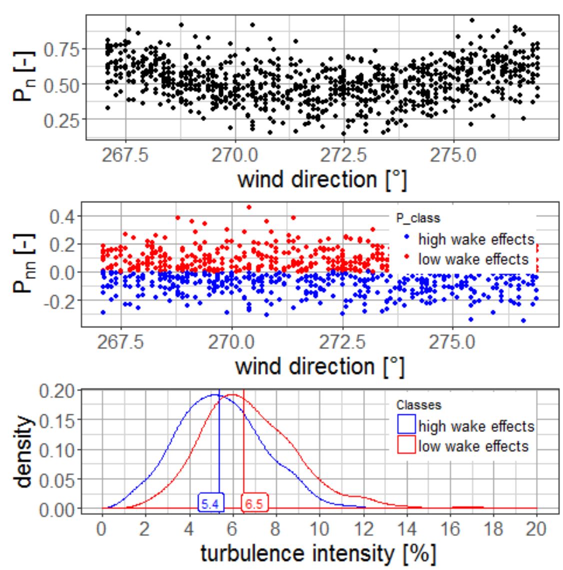

Figure 5: a) Power of AV5 normalized with the power of AV4 for 10° sector around the full wake for wind speed range 8 ± 1 m/s. b) Wind direction dependency corrected normalized power. Each 2° bin is normalized with its bin average. Data is classified in high and low wake effects. c) Density distribution of the turbulence intensity from the met mast for each data subset with median.

~~First, the power of a turbine in the wake is normalized with the power of a turbine in free flow conditions. This normalized power from a narrow sector of 10° centred at the full wake is divided into three groups. Medium wake effects are ±5 % around the median of the normalized power. High wake effects are 5 % below and low wake effects are 5 % above the median of the normalized power. In the second step the density distribution of the new SCADA signal is plotted for all three groups and the thresholds are selected to achieve best distinction between the three data sets.~~The third step divides the data set into high wake effects (values < 0) and low wake effects (values >= 0). The median of each data subset is proposed to allocate the thresholds (See Fig. 5c).

Kommentar [RC1-10]: - §3.3 New classification and validation. This part is confusing. The authors determine a classification of the wake effect on the basis of the median of the normalized power of a wind turbine in wake interaction. It means that the intensity of the wake effect is determined by its statistical occurrence and not by its strength. Please elaborate an argumentation to justify this strategy of classification

Formatiert: Standard

Formatiert: Englisch (USA)

Formatiert: Nicht vom nächsten Absatz trennen

Formatiert: Beschriftung

Kommentar [RC2-11]: Page 7, line 26 Why use the median instead of the mean?

Kommentar [RC2-12]: Page 8, line 2 '...the thresholds are selected to achieve the best distinction between the three data sets.' As these thresholds are central to the stability classification (and this work in general), a mathematical definition of best distinction must be included. Currently, this work is unreproducible by a third party.

~~The quality of the established relationship in terms of dependency on turbine type, layout and location of the wind farm is tested by applying the same classification on a different wind farm where no met mast is available.~~

Formatiert: Beschriftung

4 Results and Discussion

4.1 Stability and t~~T~~urbulence ~~stability~~ intensity classification ~~and its impact on power production~~

For the selected period at alpha ventus, Fig. 6 shows the stability distribution with the proposed thresholds of $\zeta = 33/L$ from Table 1. There is a clear tendency of having more stable conditions with increasing wind speed. This trend is also visible with turbulence intensity measured at FINO1. The strong wind speed dependency of PO_{TI} leads to an overestimation of this behaviour. The proposed normalization as described in Eq. (6) reduces this information.

Formatiert: Englisch (USA)

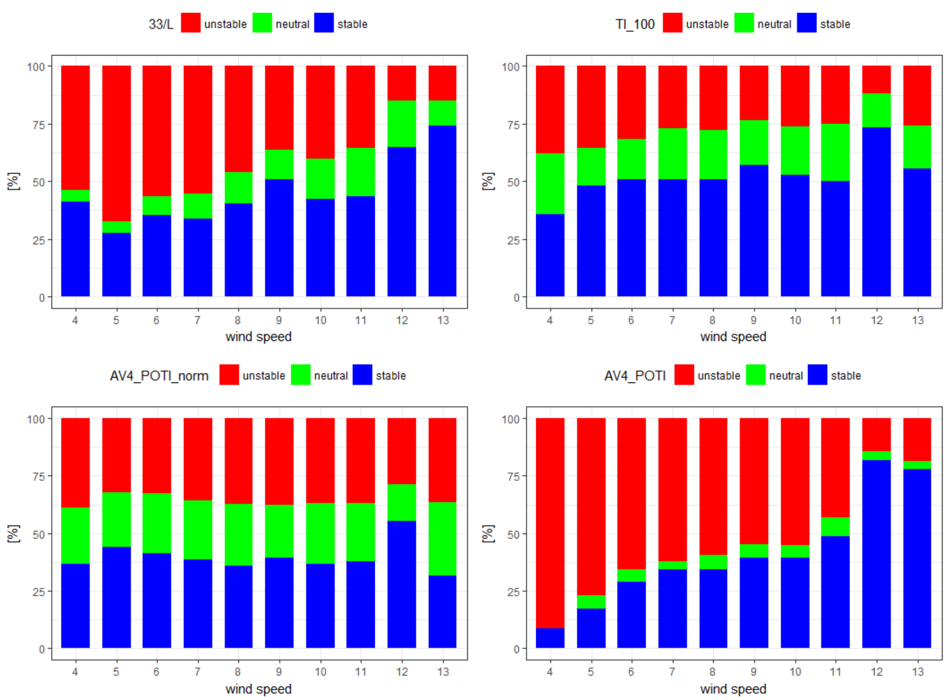

Figure 6: Distribution of stability based on ζ as a function of wind speed for different parameters of interest.

Figure 7 presents the data from FINO1 with bin averaged met mast turbulence intensity measured at 100 m (TI_100), turbulence intensity from the turbines nacelle anemometer at hub height (AV4_TI), power law coefficient from 40 m and 90 m heights (alpha_40_90) and the standard deviation of the power divided by the average power (AV4_POTI). Each signal is plotted as function of the wind speed for the three proposed stability classes based on $\zeta = \frac{33}{L}$.

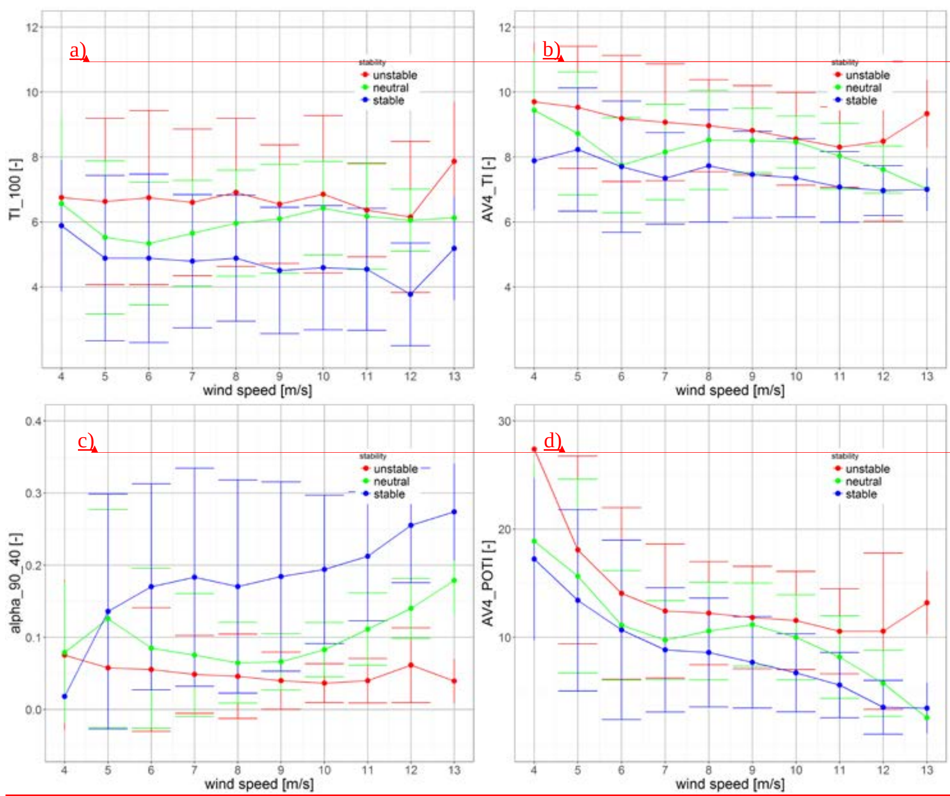

Figure 7: a) Turbulence intensity at FINO1, b) Turbulence intensity at AV4, c) Power Law coefficient for shear at FINO1 hights at 40m and 90m and d) Standard deviation of the power divided by the average power for free flow conditions at AV4. All four measurements are provided as function a of the wind speed for three stability classes based on $\zeta = \frac{33}{L}$.

For all signals in Fig. 7 the differences between the stability classes is visible. Whereas shear (See Fig. 7c) has problems in light winds, it gives the best results for the higher wind speeds. Turbulence intensity (See Fig. 7a) is the most constant signal for the selected wind speed range. The turbulence intensity measured at the nacelle (See Fig. 7b) is much higher due to the location of the anemometer behind the rotor. This comprises the variation and weakens the ability to distinguish between the stability classes. The relationship between the standard deviation of the power divided by the average power (See Fig. 7d) and the wind speed is very dominant and can be approximated with a third order polynomial.

Formatiert: Deutsch (Deutschland)

Formatiert: Deutsch (Deutschland)

Formatiert: Deutsch (Deutschland)

Formatiert: Deutsch (Deutschland)

4.2 Impact on power production

Alpha ventus data from almost four years of operation is used to evaluate the influence of atmospheric stability ~~estimated from the~~and turbulence intensity ~~and its influence~~ on the wake development. Figure 8~~Figure 5~~ ~~proves~~ shows the different wake ~~behaviour~~behaviour under different turbulence conditions. The top row of plots ~~shows~~ are~~the~~ single wake condition of turbine AV5 in the wake of AV4. The second row displays the same evaluation but for the double wake condition of AV6 in the wake of AV4 and AV5. The left side is a normalised power deficit as function of the wind direction for a wind speed range from 7 m/s to 9 m/s. On the right side, there is the normalised power as function of the wind speed for a sector width of 10 °. Each graph states the total number N of data points which have been split into stable (blue dots), neutral (green diamonds) and unstable (red triangles) data sets. Each symbol is the average of a 2 ° bin (2 m/s bin) and the error bars indicate the standard error of the mean.

For the single wake, a clear distinguishable difference between the stable and unstable power deficit is visible. The largest deviation is found in the full wake. The second wake has a less pronounced difference in power which can be explained by the fact, that the first turbine operating in the wake supports the mixing with the ambient wind speed. Another interesting effect is noticeable in the top left plot. The difference in power for the different stabilities is higher at the right hand side of the deficit in downstream direction. This right drift of the wake in stable conditions has also been observed in LES simulations by Vollmer et al.(2016). This effect is even more pronounced when the data is distinguished with $\zeta = 33/L$ (See Fig. 9). The total magnitude of wake effects is better distinguished by the classification with turbulence intensity. For this reason we will consider from now on turbulence intensity as reference.

The turbulence intensity for this classification has been measured at 100 m which is the largest height at the FINO1 met mast. The second height of the FINO1 met mast (90 m) is closer to hub height (92 m), but the strong mast structure and the boom orientation of 135 ° cause~~s~~ disturbance for wind directions within the selected sector for our investigation. No further correction, e.g. to account for the difference in height was necessary according to the findings of Tuerk (2008).

For the wind farm Nordsee Ost (NO) only one full year of SCADA data and six month of LiDAR data is available for this investigation. ~~Fifteen~~ Eighteen PPI scans (as described in ~~Section~~Sect. 2.5) ~~at wind direction from 236 ° - 242 °~~with full wake conditions are available and categorized according to the classification in Table 1~~Table 1~~. Fig. 10~~6~~ displays the wind speed measured with the LiDAR normalized with the inflow wind speed measured at the met mast. The wind speed recovers faster for the unstable turbulence class than for the neutral and stable class. The second and third turbine in the row for the investigated wind direction are marked with blue vertical lines. The decreased wind speed in the induction zone in front of each downstream turbine is clearly visible. The error bars indicate the standard error of the mean. For the stable class $TI \leq 4\%$ only one set of PPI scans is available.

Formatiert: Überschrift 2

Kommentar [RC2-13]: Page 8, line 7 Please avoid use of the word 'prove' in this context.

Formatiert: Englisch (USA)

Formatiert: Englisch (USA)

Feldfunktion geändert

Formatiert: Englisch (USA)

Formatiert: Englisch (USA)

Formatiert: Englisch (USA)

Formatiert: Englisch (USA)

Formatiert: Englisch (USA)

Feldfunktion geändert

Formatiert: Englisch (USA)

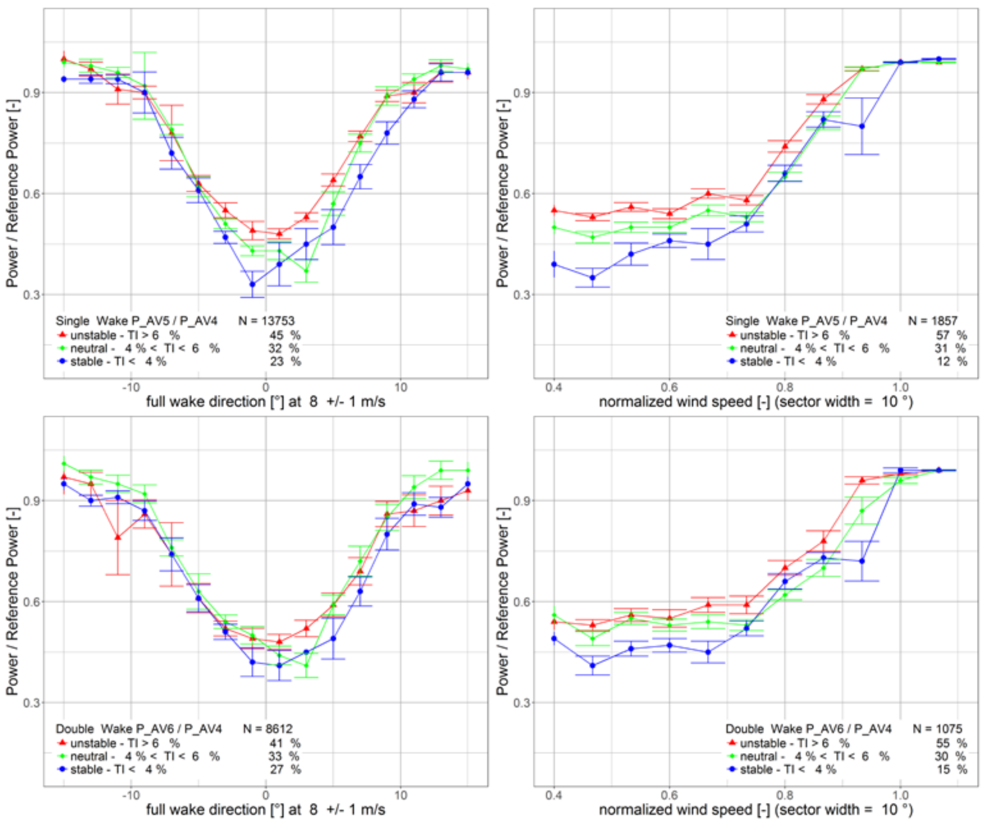

Figure 8: Wake effects in alpha ventus (AV) under different atmospheric conditions classified by met mast turbulence intensity. Power of downstream turbine normalised with free flow turbine. Upper row: single wake, bottom row: double wake. Left column: Normalised Power as function of wind direction, right column: Normalised power as function of wind speed.

Kommentar [RC2-14]: Page 9, fig 5, bottom left One point just right of the centre for the stable curve is clearly an outlier. Any comment? Tables 2–5 The large variation in thresholds suggests that the approach is not general and more details regarding how these thresholds are determined is needed.

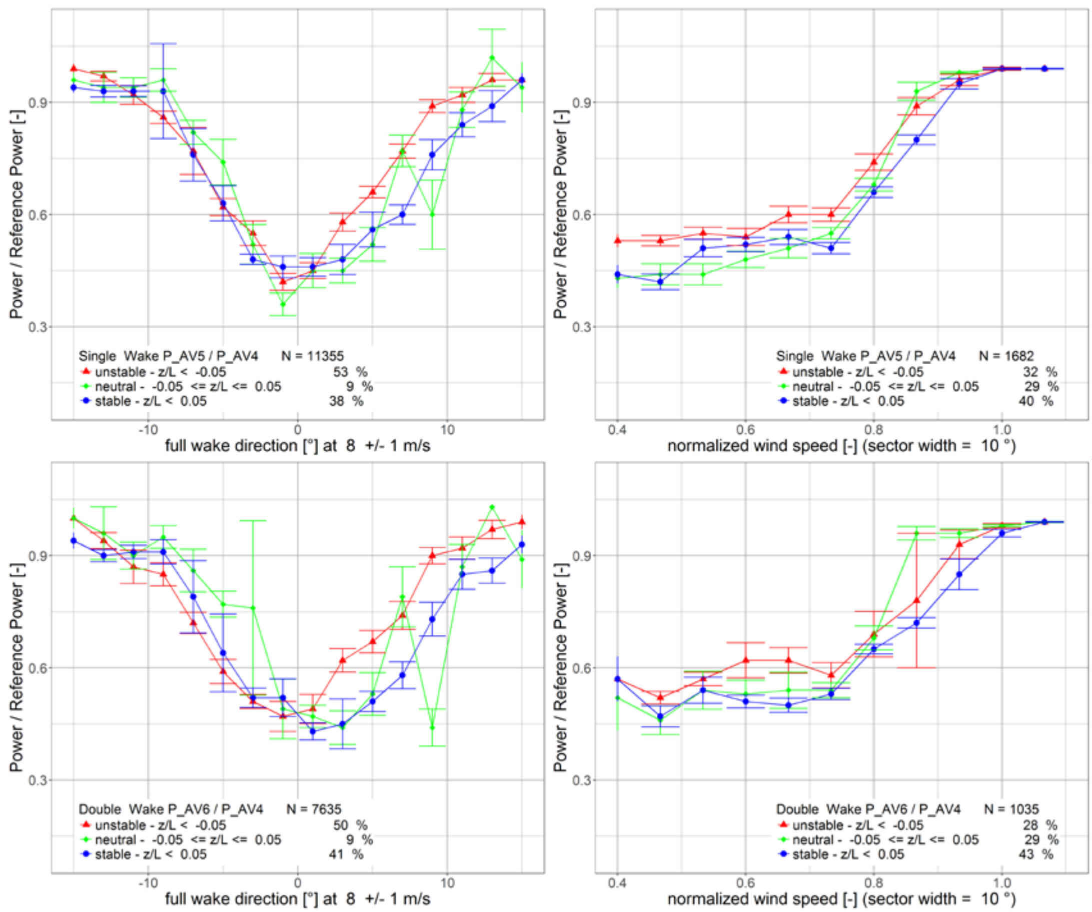

Figure 9: Wake effects in alpha ventus (AV) under different atmospheric conditions classified by $\zeta = 33/L$. Power of downstream turbine normalised with free flow turbine. Upper row: single wake, bottom row: double wake. Left column: Normalised Power as function of wind direction, right column: Normalised power as function of wind speed.

Formatiert: Nicht vom nächsten Absatz trennen

Kommentar [RC2-15]: Page 9, fig 5, bottom left One point just right of the centre for the stable curve is clearly an outlier. Any comment? Tables 2–5 The large variation in thresholds suggests that the approach is not general and more details regarding how these thresholds are determined is needed.

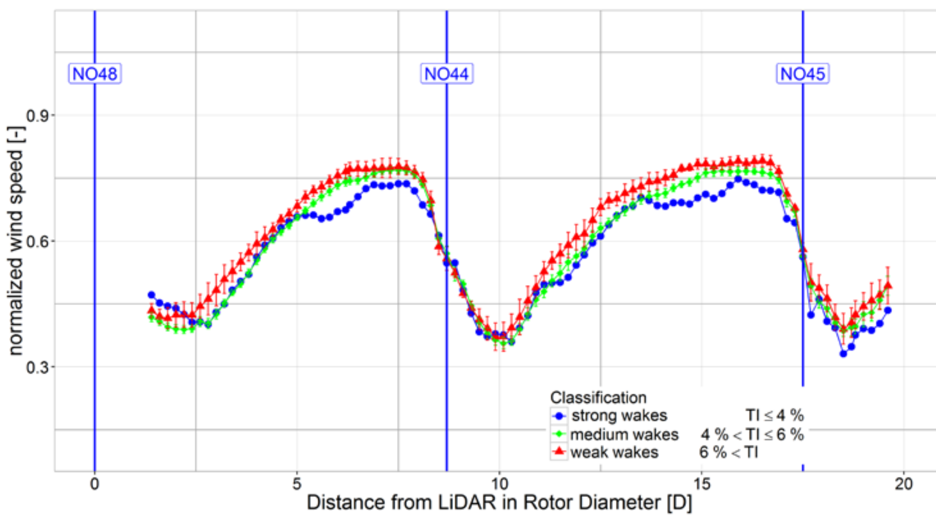

Figure 10: Wind speed recovery at wake centre on hub height behind NO48 for different turbulence stability classes. The wind speed is normalized with the inflow wind speed and the distance from the LiDAR on NO48 downstream is displayed in multiples of rotor diameters

4.3~~2~~ Correlation analysis

In the next step, we correlate the SCADA signals described in ~~Section~~Sect. 3.2 with the turbulence intensity measured at the mast. In Fig. 7 a panel plot is displayed. The graphs on the diagonal present the histogram and density distribution for the respective variable. The panels above the diagonal provide the Pearson correlation coefficients. The lower panels are scatter plots for the two variables with a fitted linear regression line. The colours of the points indicate the three stability classifications (blue: stable, green: neutral, red: unstable) determined with the met mast turbulence intensity.

The correlation between met mast and turbine TI in subplot (1 , 2) equals to 0.55. This poor result can be explained by the nacelle wind speed measurement position behind the rotor, which induces additional disturbance to the flow.

The highest correlation with the met mast TI is obtained with the standard deviation of the turbine power divided by its average active power ($PO_{TI,AV4}$) in subplot (1 , 5). Although a correlation of 0.66 is not perfect, it is still better than the turbulence measured with the nacelle cup anemometer. Especially in the low turbulence region, the scatter plot proves to be denser. Very similar results are obtained when applying the same analysis to AV1 and AV2.

Kommentar [RC1-16]: - §4.2 Correlation analysis. It is not clear whether the data are sorted only according to the turbulence intensity or also to the wind speed (as performed in Fig. 5). If the data are not sorted according to the wind speed, it means that different operating conditions are plotted without distinction in this correlation matrix. How can one expect to get strong correlations between data coming from the incoming flow conditions (fully independent of the operation parameters) and operation-driven data coming from the wind turbines without any additional filters ? Could you please show the evolution of the relative power fluctuation PO_TI with the WT power or with the wind speed? Regardless of this crucial point, one cannot state that the level of correlation is acceptable in order to use this information as a representation of the turbulence intensity, and even less of the atmospheric stability.

Kommentar [NM17]: Please find the requested plot in Fig.7. The filtering is described in Sect. 2.4.

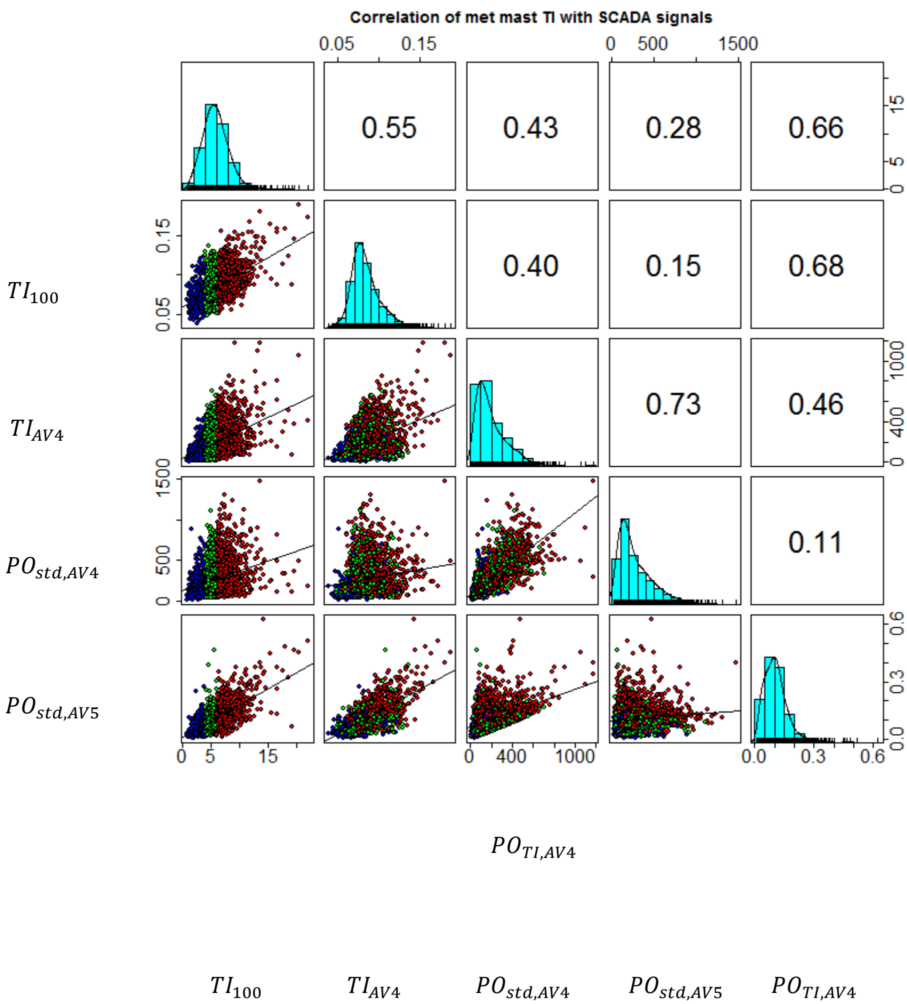

Figure 11: Correlation matrix. Turbulence intensity from met mast (TI_{100}) is correlated with the TI measured with the nacelle anemometer of AV4 (TI_{AV4}), the standard deviation of the 10 min power of AV4 ($PO_{std,AV4}$), the standard deviation of the 10min power of AV5 ($PO_{std,AV5}$) and the standard deviation of the power divided by the average power of AV4 ($PO_{TI,AV4}$). All dimensions are in [%] except for the standard deviation of the power which is in [kW].

To check the validity of these results, we use data from Nordsee Ost (NO). ~~Figure 8~~Figure 12 provides the information corresponding to Fig. ~~7~~11 but for a different turbine type, met mast and a different location in the North Sea.

The correlation reveals the best result for the $PO_{TI,NO47}$signal (0.62). TI_{NO47} derived from the nacelle cup anemometer gives 0.60 . The difference between these two signals is much smaller than in alpha ventus. A different blade design and the distinct turbine nacelle met mast layout might be the reason for this.

Both correlation analyses show that the new artificial SCADA signal, derived from the standard deviation of the power divided by its average active power PO_{TI} is the most suitable among the selected signals to substitute a met mast TI_{mast} for our purpose. In the next ~~section~~Section, we check the influence of this new signal on the estimated power production in the wake.

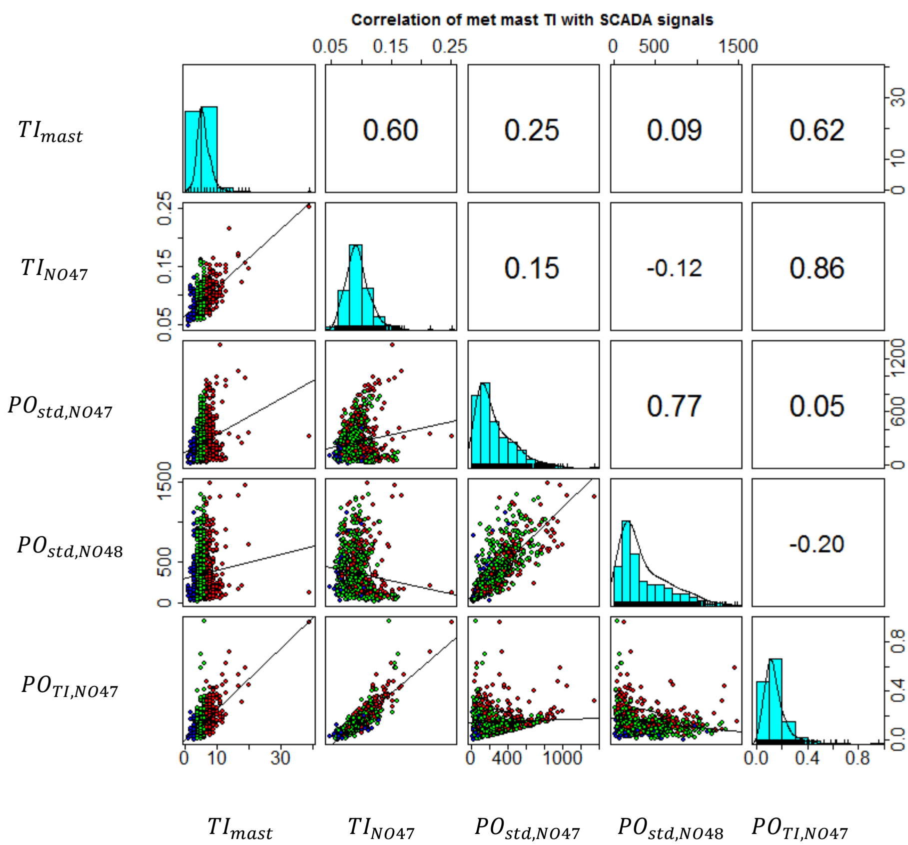

Figure 12: Correlation analysis for Nordsee Ost. Turbulence intensity (TI_{mast}) measured at hub height is correlated with the TI measured with the nacelle anemometer of NO47 (TI_{NO47}), the rotor estimated wind speed ($TI_{NO47_{u_{es}}}$), the standard deviation of the 10 min power of NO47 ($PO_{std,NO47}$), the standard deviation of the 10 min power of NO48 ($PO_{std,NO48}$), the standard deviation of the power divided by the average power of NO47 ($PO_{TI,NO47}$). All dimensions are in [%]except for the standard deviation of the power which is in [kW].

4.~~3~~ 4 New classification and validation

In ~~Section~~Sect. 4.2 we demonstrated the correlation of the SCADA signal ~~(~~PO_{TI}~~)~~ ~~derived by the standard deviation of the power divided by its average power~~ with the turbulence intensity measured at a met mast in free flow conditions. In Fig. 7d a strong wind speed dependency for the range of interest prevents a constant threshold establishment. Therefore the adjustment with Eq. (6) is proposed. Figure 13 shows $PO_{TI_{norm}}$ as a function of wind speed for the three stability classes based on ζ. The error bars are 1 standard deviation.

For AV4 the constants of the third order polynomial are $\beta_0 = 99.9,\ \beta_1 = -32.5,\ \beta_2 = 3.9$ and $\beta_3 = -0.16$.

.

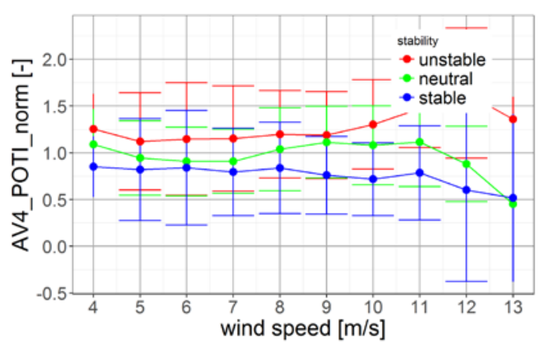

Figure 13: Normalized SCADA signal ($PO_{TI_{norm}}$) for the classification of the magnitude of wake effect.

Formatiert: Nicht vom nächsten Absatz trennen

Formatiert: Beschriftung

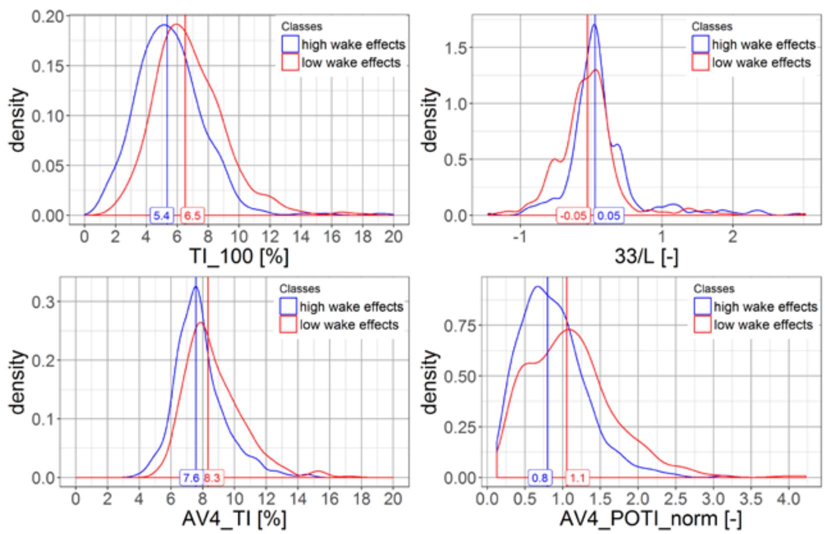

Figure 14: The thresholds are displayed as vertical lines representing the median of the density distribution for the signal of interest.

With the methodology from Sect. 3.3 we obtain different density distributions for high and low wake effects (See Fig. 14). The thresholds are derived from the median of the data distribution. For ζ we obtain exactly the same values as proposed in Table1.

Comparing the two turbulence intensities in Fig. 14 a) and c) one can clearly see the increased turbulence behind the rotor especially for low TI values. The distribution for the nacelle measurement is compressed in a way, that the low measurements have up to 4% difference but the high turbulence intensities are more or less comparable. This effect reduces the ability of the nacelle turbulence intensity to distinguish between the wake magnitude. A more clear separation between the wake classes can be achieved with the new proposed $PO_{TI_{norm}}$.

The quality of the established relationship in terms of dependency on turbine type, layout and location of the wind farm is tested by applying the same classification on a different wind farm where no met mast is available.

In the next ~~step~~Sections, the ability of this new signal to distinguish between different environmental stratification is analysed. Table 2 ~~Table 2 to Table 5~~ shows the proposed thresholds for the different parameters under investigation.

Table 2: Summary of thresholds for the different classes of interest at alpha ventus:

Category	$\zeta = z/L$ [-]	TI_{100} [%]	$AV4_{TI}$ [%]	$AV4\_POTI_{norm}$ [-]
Weak wakes	$\zeta < -0.05$	$TI_{100} > 6.5$	$AV4_{TI} > 6.5$	$POTI_{norm} < 0.8$

Formatiert: Englisch (USA)
Formatiert: Englisch (USA)
Formatiert: Englisch (USA)
Formatiert: Englisch (USA)
Feldfunktion geändert

Medium wakes	$-0.05 \leq \zeta \leq 0.05$	$5.4 \leq T_{100} \leq 6.5$	$5.4 \leq AV4_{TI} \leq 6.5$	$0.8 \leq POTI_{norm} \leq 1.1$
Strong wakes	$\zeta > 0.05$	$T_{100} < 5.4$	$AV4_{TI} < 5.4$	$POTI_{norm} > 1.1$

~~classifications for each wind farm (also corresponding to different turbine types).~~

4.~~3~~4.1 alpha ventus (AV)

The classification of wake effects by the $PO_{TI_{norm}}$ signal is illustrated in Fig. ~~9~~15 analogous to Fig. ~~5~~ 8 where the turbulence intensity TI_{mast} is used.

Kommentar [RC1-18]: - §4.3.1 New classification and validation on Alpha Ventus. By applying the new classification; discrepancies in the power production due to the assessed stability is rather small and difficult to interpret. By comparing Fig 5 and Fig 9, one notice that the frequency of occurrence of each stability class is also totally dependent of the classi- fication method. For instance, on the top-right plot, the unstable case occurrence is 13% of samples for the new classification, instead of 56% with the classification based on turbulence intensity. It show again the poor correlation between both information.

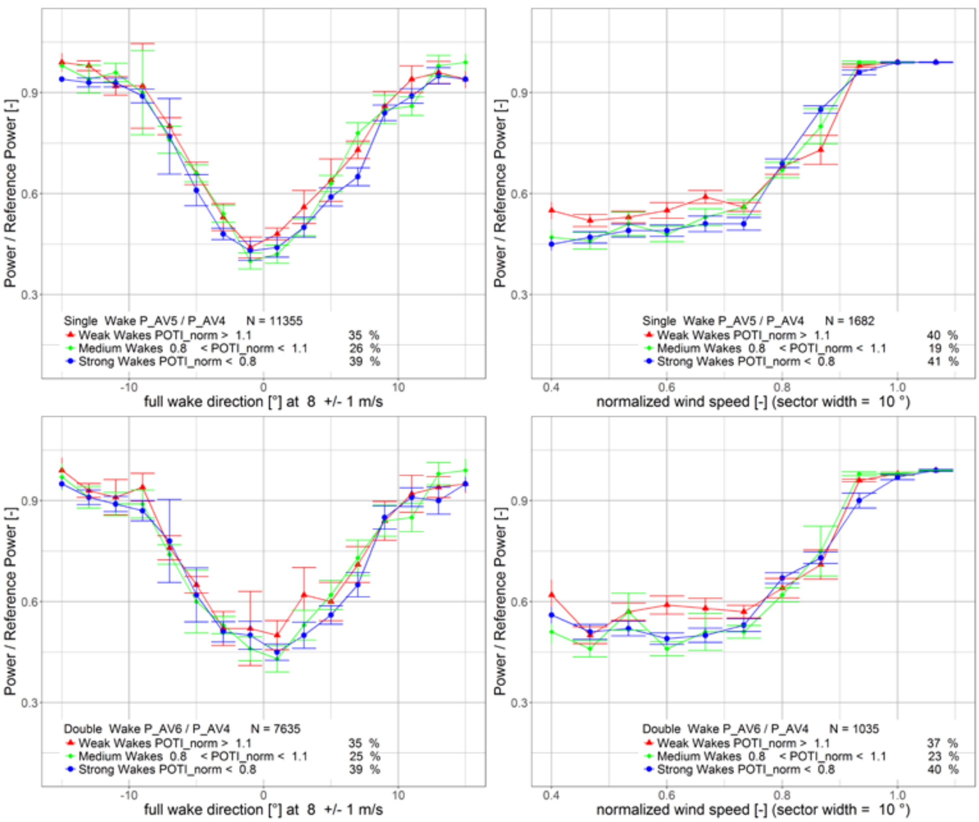

Figure 15: Stability classification with the $PO_{TI_{norm}}$ value. Power of waked turbine normalised with free flow turbine. Upper row: single wake, bottom row: double wake. Left column: Normalised Power as function of wind direction, right column: Normalised power as function of wind speed.

A clear difference in power production between stable and unstable cases can be identified in the single wake. The differences in double wake are again less pronounced. Compared to the TI classification, the curves for the neutral case are not as clear as in-between the stable and unstable curves and in the normalized power curve plots (right column) the stable conditions can only be highlighted up to the wind speed of rated power for the free flow turbine. This can be explained with the fact, that at rated power the pitch controller rather than the power variation is governing the turbine reaction on turbulence intensity. This leads in Eq. (4) to a significant decrease of the numerator and keeps the denominator constant.

~~**Table 2: Definition of stratification by power intensity: alpha ventus**~~

~~Classification~~	~~Power Intensity (PO_{TI})~~
~~Unstable~~	~~$PO_{TI} > 13\ \%$~~
~~Neutral~~	~~$13\ \% \geq PO_{TI} \geq 7\ \%$~~

~~Stable~~	~~7 % > PO_{TI}~~

4.~~3~~4.2 Nordsee Ost (NO)

The classification of wake effects in Fig. ~~10~~ 16 is based on PO_{TI_norm} and analogous to Fig. ~~6~~ 10 where turbulence intensity TI_{mast} ~~has been~~is used. For these plots the Gaussian fitted minima's of the normalized wind speed (wake centres) measured by the LiDAR are plotted for each distance behind NO48.

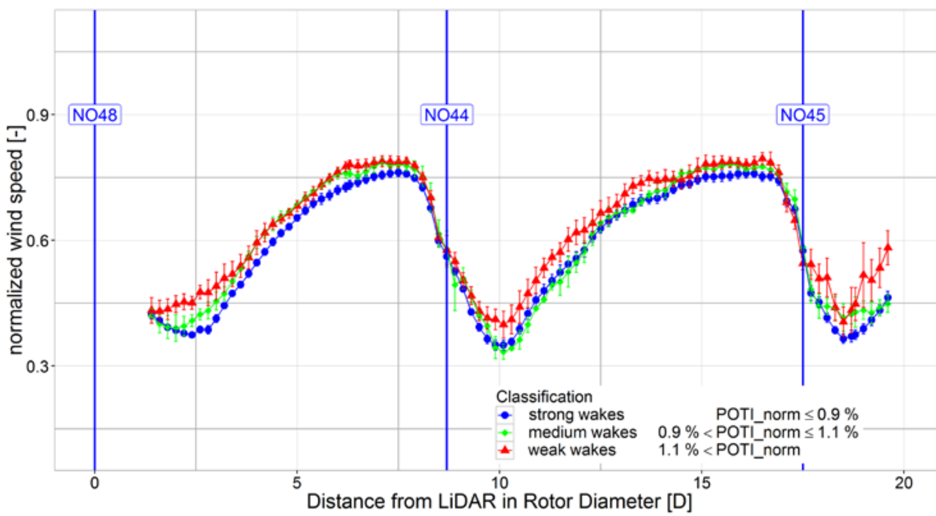

Figure 16: Wind speed recovery behind NO48 for different $PO_{TI_{norm}}$ classes. The wind speed is normalized with the inflow wind speed and the distance from the LiDAR on NO48 downstream is displayed in multiples of rotor diameters.

~~Again, t~~This result states ~~stronger wake effects for stable cases compared to unstable situations~~the ability of $PO_{TI_{norm}}$ to distinguish between different wake effects. The single wake has a less pronounced difference between the three classes and the slope of the wind speed recovery is smaller than the double wake case. E.g. 5D behind the first turbine, the wind speed has recovered to approximately 70% of the free flow wind speed and in the second wake 5D behind NO44 we see already more than 75%. This fact leads to the performance increase at the third turbine (NO45) compared to the second turbine (NO44). Wake added turbulence of NO48 is helping to recover the wind speed.

~~**Table 3: Definition of stratification by power intensity: Nordsee Ost**~~

~~Classification~~	~~Power Intensity (PO_{TI})~~
~~Unstable~~	~~PO_{TI} > 16 %~~
~~Neutral~~	~~16 % ≥ PO_{TI} ≥ 12 %~~
~~Stable~~	~~12 % > PO_{TI}~~

4.~~3~~4.3 Ormonde (OR)

Finally the transferability of classification boundaries to other wind farms where no met mast is available is of interest. First we have a look at the sensitivity of the ~~proposed~~ signal PO_{TI} in terms of turbulence from neighbouring turbines and wind farms. In Fig. ~~11~~17, the directional bin averaged PO_{TI} from OR24 is able to identify the location of its neighbours. The magnitude allows to determine which turbine is next (OR25 at 4.2D) and which is further away (OR22 at 6.7D, OR23 at 6.6D and OR21 at 9.1D).

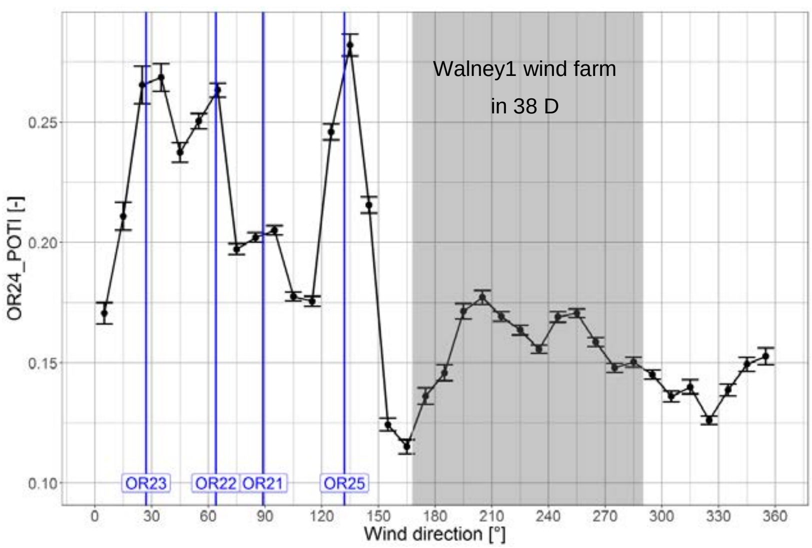

Figure 17: The ~~new proposed~~ signal PO_{TI} is sensitive to wake-induced turbulence from neighbouring turbines and wind farms. With PO_{TI} from turbine OR24 it is even possible to rank the distance of the neighbours being OR25 the closest with 4.2D and OR21 the farthest with 9.1D.

The grey area represents the geometrical location of the neighbouring wind farms Walney 1 and 2. The closest distance to OR24 has Walney 1 with approximately 38.8D (SWT-3.6-107 Siemens). The two peaks at 208° and 255° are wind directions for which multiple turbines of the neighbouring wind farm are aligned in a clear row of full wake situations. The increase from 345° to 15° can be explained with the coastline that gets quickly closer in clockwise direction.

Secondly we have a look at the influence on the wake recovery. With south westerly wind direction, we focus on single wake, double wake and triple wake conditions behind turbine number OR27 for a sector of 10° around the full wake situation. And for north westerly wind directions we investigate the rows of turbines behind OR23. The main differences between these two directions are the average level of inflow turbulence intensity and the different spacing between the turbines. In Fig. 17 ~~11~~, the inflow turbulence level from north west (sector of 302 ° to 322 °) is much lower (bin average

$\overline{PO_{TI}} \approx 12.5$ %) than from south west (sector of 192 ° to 222 °, bin average $\overline{PO_{TI}} \approx 17.5$ %) due to the wake effects from Walney 1 in more than 38D distance.

~~It was not possible to use exactly the same thresholds for the classification which is on the one hand a result of the usage of different turbines and controller versions in alpha ventus, Nordsee Ost and Ormonde. On the other hand there seems to be a dependence on the ambient turbulence level. Table 4 and Table 5 provides the new thresholds for the different classifications in Ormonde, estimated as described in Section 3.3.~~

Formatiert: Deutsch (Deutschland)

Formatiert: Deutsch (Deutschland)

Formatiert: Deutsch (Deutschland)

Formatiert: Deutsch (Deutschland)

Feldfunktion geändert

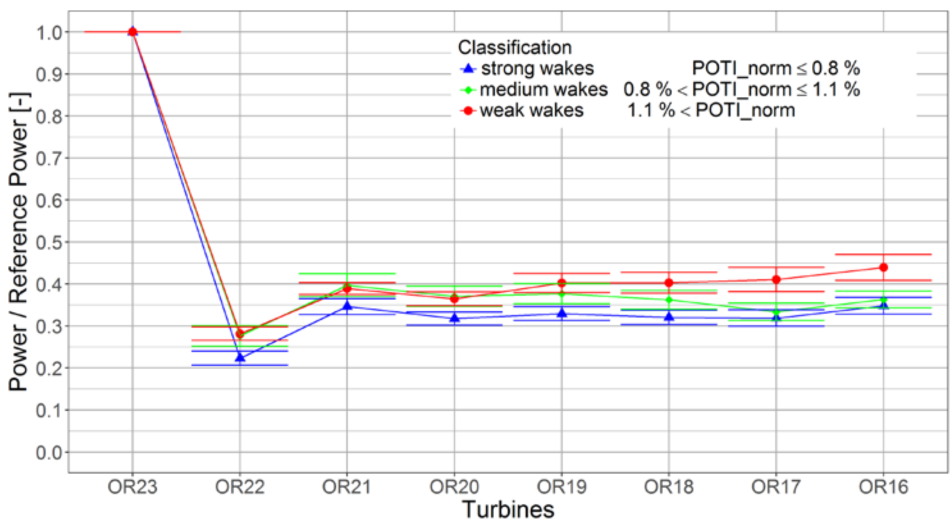

Figure 18: Normalized power for each turbine along the row behind OR23 for a wind direction of 312 ° and a 10 ° sector width and 8 m/s ±1. Stability classes distinguished with the signal $PO_{TI_{norm}}$ from OR23.

For north westerly wind direction, Fig. 18 ~~12~~ provides a view on different wake effects for the proposed classification~~at different stability classes~~. The normalized power for each turbine in the row behind OR23 is displayed (wind from left to right). Wind speed is filtered for 8 ± 1 m/s~~7 – 9 m/s~~ and the wind direction is 316~~2~~ ° with a sector width of 10 °. The largest wake effects are detected at OR22. This underlines the observation from the LiDAR measurements in NO. The first wake is the strongest and all consecutive wakes are better mixed due to wake added turbulence. The difference in power production between ~~stable~~ high and ~~unstable~~ low turbulence conditions~~cases~~ is in the range of 10%, which also demonstrates the importance of this effect for wake model developers to take it into account.

The south westerly wind direction is analyzed in Fig. 19 ~~13~~, which is a similar illustration as Fig. ~~5~~ 8 and Fig. 9. ~~The PO_T signal is on a higher level due to the wind farm wake effects from Walney 1 and 2.~~ It is still possible to identify different wake behaviour for the different classes but the effect is less pronounced than in the previous examples. A higher

Kommentar [RC2-19]: Page 16, line 19 Why limit the data set to 7–9 m/s? Are these results representative?

Kommentar [RC2-20]: Page 17, line 1 ‘The difference in power production between stable and unstable cases is in the range of 10%.’ Stability is only inferred here from TI so the statement should preferably refer to differences between high and low TI conditions.

level of inflow turbulence intensity contributes to the mixing of the wake with free wind. Hence at lower inflow turbulence levels the effect of the wake added turbulence is larger.

Further investigations are necessary to account for controller properties and to fill the normalized wind speed range [0.75 – 1], beyond the rated wind speed of the turbine in free flow conditions.

~~**Table 4: Definition of stratification by power intensity: Ormonde for south westerly winds**~~

~~Classification~~	~~Power Intensity (PO_{TI})~~
~~Unstable~~	~~$PO_{TI} > 18\ \%$~~
~~Neutral~~	~~$18\ \% \geq PO_{TI} \geq 13\ \%$~~
~~Stable~~	~~$13\ \% > PO_{TI}$~~

~~**Table 5: Definition of stratification by power intensity: Ormonde for north westerly winds**~~

~~Classification~~	~~Power Intensity (PO_{TI})~~
~~Unstable~~	~~$PO_{TI} > 9\ \%$~~
~~Neutral~~	~~$9\ \% \geq PO_{TI} \geq 7\ \%$~~
~~Stable~~	~~$7\ \% > PO_{TI}$~~

In performance monitoring of offshore wind farms the newly aggregated SCADA signals can be used as an auxiliary quantity to classify different atmospheric ~~stability~~ conditions. Advanced engineering wake models which are able to take turbulence intensity or stability parameters into account, may be parameterized by these artificial turbine signals in order to improve their prediction of wind turbine power production under waked conditions.

Kommentar [RC2-21]: Page 17, line 8 The paper would be significantly more complete with this range of important wind speeds included in the analysis.

Kommentar [RC1-22]: - The thresholds used in the new classification are different for each tested wind farms. It is justified by the fact that the wind turbines are different. But how can one explain that thresholds are different on the same wind farm (Ormonde) but for different wind directions?

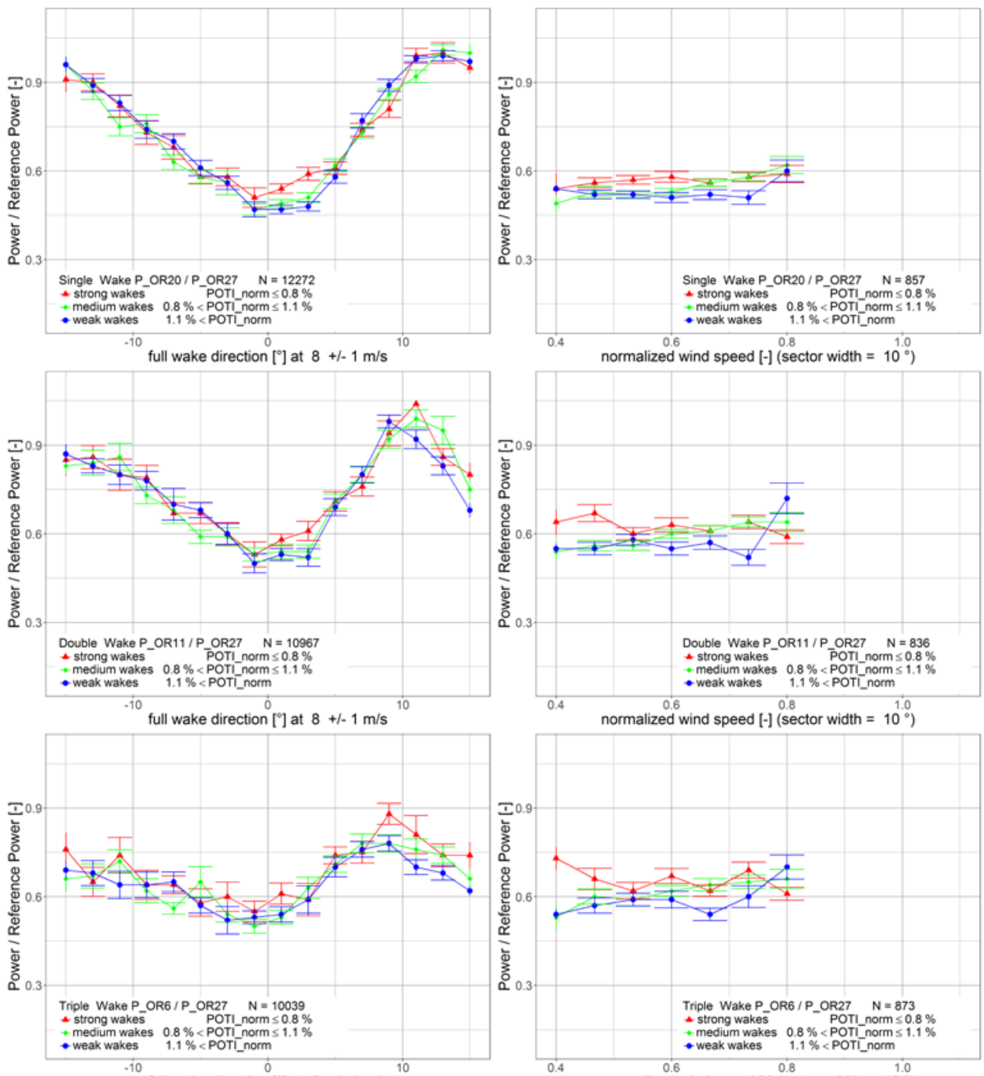

Figure 19: Wake effects in Ormonde (OR) under different ~~atmospheric~~ conditions. Power of downstream turbine normalised with free flow turbine. First row: single wake, second row: double wake and third row: triple wake. Left column: Normalised Power as function of wind direction, right column: Normalised power as function of wind speed.

5 Conclusions

Measured data from three different offshore wind farms, two met masts, one buoy and one long range LiDAR has been analysed to identify different influence on power production at turbines operating in the wake. We have validated the method described in Dörenkämper (2015), which proposes to use the turbulence intensity, to describe the power production in the wake and compared it with the atmospheric stability evaluation proposed by (Ott and Nielsen, 2014).~~.~~ In this case, turbulence intensity could better distinguish between the magnitude of wake effects. A correlation analysis was performed and for wind speeds in partial load operation, the standard deviation of the power divided by its average power (PO_{TI}) was identified having similar behaviour than the turbulence intensity. A sensitivity check for PO_{TI} ~~reviled~~ revealed very detailed responsiveness to increases in turbulences due to neighbouring turbines and wind farms. Effects from wind farm neighbours are detectable even more than 38 rotor diameter away. A strong wind speed dependency of this signal can be eliminated by normalization with a third order polynomial fitted to the data. A classification of different turbine behaviour based on this adjusted $PO_{TI_{norm}}$ was analysed and compared to the classification with turbulence intensity TI.

Both signals can distinguish between stronger and weaker wake effects. ~~A transferability of the findings from one turbine to the next is only possible under the prerequisite of having the same turbine type and controller version.~~ The magnitude of influence of the $PO_{TI_{norm}}$ signals on wake effects is dependent on the level of inflow turbulence intensity. Higher inflow turbulence has already a higher wake mixing and therefore the wake added turbulence has a less pronounced contribution.

Using $PO_{TI_{norm}}$ to predict wakes more accurate is a promising approach, but further investigations are necessary to take controller properties into account ~~and~~ to fill the wind speed range beyond the rated wind speed of the turbine in free flow conditions.

Kommentar [RC2-23]: Page 18, line 7 Typo: 'reviled' should be 'revealed'.

Acknowledgements

The presented work is partly funded by the Commission of the European Communities, Research Directorate-General within the scope of the project "ClusterDesign" (Project No. 283145 (FP7 Energy)). We would like to thank Deutsche Offshore-Testfeld und Infrastruktur GmbH & Co. KG (DOTI), Research at alpha ventus (RAVE), Forschungsplattformen in Nord und Ostsee (FINO1), Innogy SE, Vattenfall Wind Power and Senvion SE for making this investigation possible. Furthermore a special thanks to the R Core Team for developing the open source language R (R_Core_Team, 2015).

References

Archer, C. L., Colle, B. A., Veron, D. L., Veron, F. and Sienkiewicz, M. J.: On the predominance of unstable atmospheric conditions in the marine boundary layer offshore of the U.S. northeastern coast, J. Geophys. Res. Atmos., 121(15), 8869–

8885, doi:10.1002/2016JD024896, 2016.

Beck, H., Trabucchi, D., Bitter, M. and Kühn, M.: The Ainslie Wake Model An Update for Multi Megawatt Turbines based on State-of-the-Art Wake Scanning Techniques, in Proceedings of the European Wind Energy Association, Barcelona, Spain, 10-13 March., 2014.

Dörenkämper, M.: An investigation of the atmospheric influence on spatial and temporal power fluctuations in offshore wind farms, PhD Thesis, University of Oldenburg, Oldenburg., 2015.

Dörenkämper, M., Tambke, J., Steinfeld, G., Heinemann, D. and Kühn, M.: Influence of marine boundary layer characteristics on power curves of multi megawatt offshore wind turbines, in Proceedings of 11th German Wind Energy Conference, Bremen, Germany, 7-8 November., 2012.

Dörenkämper, M., Tambke, J., Steinfeld, G., Heinemann, D. and Kühn, M.: Atmospheric Impacts on Power Curves of Multi-Megawatt Offshore Wind Turbines, J. Phys. Conf. Ser., 555(1), 12029, doi:10.1088/1742-6596/555/1/012029, 2014.

Göçmen, T. and Giebel, G.: Estimation of turbulence intensity using rotor effective wind speed in Lillgrund and Horns Rev-I offshore wind farms, Renew. Energy, 99, 524–532, doi:10.1016/j.renene.2016.07.038, 2016.

Hamilton, N.: Functions Relating to the Smoothing of Numerical Data, CRAN R, 1–5, 2015.

Hansen, K. S., Barthelmie, R. J., Jensen, L. E. and Sommer, A.: The impact of turbulence intensity and atmospheric stability on power deficits due to wind turbine wakes at Horns Rev wind farm, Wind Energy, 15(1), 183–196, doi:10.1002/we.512, 2012.

Iungo, G. V. and Porté-Agel, F.: Volumetric scans of wind turbine wakes performed with three simultaneous wind LiDARs under different atmospheric stability regimes, J. Phys. Conf. Ser., 524, 12164, doi:10.1088/1742-6596/524/1/012164, 2014.

Keane, A., Aguirre, P. E. O., Ferchland, H., Clive, P. and Gallacher, D.: An analytical model for a full wind turbine wake, J. Phys. Conf. Ser., 753(3), 32039 [online] Available from: http://stacks.iop.org/1742-6596/753/i=3/a=032039, 2016.

Mittelmeier, N., Blodau, T. and Kühn, M.: Monitoring offshore wind farm power performance with SCADA data and an advanced wake model, Wind Energy Sci., 2(1), 175–187, doi:10.5194/wes-2-175-2017, 2017.

Monin, A. S. and Obukhov, A. M.: Basic laws of turbulent mixing in the surface layer of the atmosphere, Inst. Contract Number, 24(19604), 163–187 [online] Available from: http://mcnaughty.com/keith/papers/Monin_and_Obukhov_1954.pdf (Accessed 21 May 2017), 1954.

More, G. and Gallacher, D.: Lidar Measurements and Visualisation of Turbulence and Wake Decay Length, in Proceedings of the European Wind Energy Association, Barcelona, Spain, 10-13 March., 2014.

Mortensen, N. G., Nielsen, M. and Ejsing Jørgensen, H.: Offshore CREYAP Part 2 – final results, European Wind Energy Association (EWEA), Helsinki, Finland, 2.Juni 2015., 2015.

Ott, S. and Nielsen, M.: Developments of the offshore wind turbine wake model Fuga, E-0046 Report 2014, DTU Wind Energy, Lyngby, Denmark., 2014.

Özdemir, H., Versteeg, M. C. and Brand, A. J.: Improvements in ECN Wake Model, in Proceedings of the ICOWES2013 Conference, Lyngby, Denmark, 17-19 June., 2013.

R_Core_Team: R: A Language and Environment for Statistical Computing, [online] Available from: https://www.r-project.org/, 2015.

Rajewski, D. A., Takle, E. S., Lundquist, J. K., Oncley, S., Prueger, J. H., Horst, T. W., Rhodes, M. E., Pfeiffer, R., Hatfield, J. L., Spoth, K. K., Doorenbos, R. K., Rajewski, D. A., Takle, E. S., Lundquist, J. K., Oncley, S., Prueger, J. H., Horst, T. W., Rhodes, M. E., Pfeiffer, R., Hatfield, J. L., Spoth, K. K. and Doorenbos, R. K.: Crop Wind Energy Experiment (CWEX): Observations of Surface-Layer, Boundary Layer, and Mesoscale Interactions with a Wind Farm, Bull. Am. Meteorol. Soc., 94(5), 655–672, doi:10.1175/BAMS-D-11-00240.1, 2013.

Sanz Rodrigo, J., Cantero, E., García, B., Borbón, F., Irigoyen, U., Lozano, S., Fernande, P. M., Chávez, R. a, Rodrigo, J. S., Cantero, E., García, B., Borbón, F., Irigoyen, U., Lozano, S., Fernande, P. M. and Chávez, R. a: Atmospheric stability assessment for the characterization of offshore wind conditions, J. Phys. Conf. Ser., 625, 12044, doi:10.1088/1742-6596/625/1/012044, 2015.

Schneemann, J., Trabucchi, D., Trujillo, J. J. and Voß, S.: Long range scanning lidar measurement campaign report, ClusterDesign Deliverable 7.1, ClusterDesign, Project No. 283145 (FP7 Energy)., 2016.

Tambke, J., Claveri, L., Bye, J. A. T., Poppinga, C., Lange, B., Bremen, L. Von and Wolff, J.: Marine Meteorology for Multi-Mega-Watt Turbines, 2005.

Tuerk, M.: Ermittlung designrelevanter Belastungsparameter für Offshore-Windkraftanlagen, PhD Thesis, Universität zu Köln., 2008.

Formatiert: Deutsch (Deutschland)

Türk, M. and Emeis, S.: The dependence of offshore turbulence intensity on wind speed, J. Wind Eng. Ind. Aerodyn., 98(8–9), 466–471, doi:10.1016/j.jweia.2010.02.005, 2010.

Vollmer, L., Steinfeld, G., Heinemann, D. and Kühn, M.: Estimating the wake deflection downstream of a wind turbine in different atmospheric stabilities: An LES study, Wind Energ. Sci, 1, 129–141, doi:10.5194/wes-1-129-2016, 2016.

Westerhellweg, A., Cañadillas, B., Kinder, F. and Neumann, T.: Wake Measurements at alpha ventus – Dependency on Stability and Turbulence Intensity, J. Phys. Conf. Ser., 555(1), 12106, 2014.

Wind Energ. Sci. Discuss., doi:10.5194/wes-2016-60-RC1, 2017

Interactive comment on

“An analysis of offshore wind farm SCADA measurements to identify key parameters influencing the magnitude of wake effects” by Niko Mittelmeier et al.

Answers to comments of anonymous Referee #1 by

Niko Mittelmeier et al. April 25, 2017

Dear Referee,
Thank you very much for reviewing our paper. Your concern, that our results are only usable for the selected wind speed bin is valid. The proposed signal is dependent on wind speed and therefore a constant threshold is limited useful. We will provide an adjustment to this fact in our answers to your comments. We will also follow your suggestion to develop the arguments in a new way. We focus on the classification of the magnitude of wake effects and show the ability to predict these conditions with the different signals. Your comments helped us to understand where we need to provide more clarity and we hope that our answers to your questions will improve the paper. Our responses to your comments are marked as ***/ Response /***.

The manuscript entitled "An analysis of offshore wind farm SCADA measurements to identify key parameters influencing the magnitude of wake effects" deals with the using of operating information supplied by the wind turbines to assess the atmospheric stability conditions and then to make some conclusions about the wake interaction effects. The objective is fully relevant: wind farms, and particularly offshore ones, are not equipped with meteorological measurements to determine the real-time and reliable meteorological conditions (wind speed, wind direction and particularly atmospheric stability). On the other hand, wind farm models need field data to be validated. The authors attempt to find an indirect way to assess atmospheric stability in order to determine the magnitude of the expected wake effects, according to this parameter.

On the other hand, the methodology used in this manuscript to obtain the presented conclusions does not sound rigorous enough at this stage to be published in a journal. Some hypothesis are too strong and the methodology is not validated.

Please find below the arguments to justify the recommendation:

- A direct correlation is expected between the turbulence intensity and the atmospheric stability. Though, for a fixed stability condition, turbulence intensity can have big scatter and particularly at low wind speeds. Reference to the works from Dörenkämper et al. (2012 and 2015) are used to justify this strong simplification but these references are a PhD thesis and a proceeding from a national conference. I would suggest to make references to publications in peer-review journals and to develop the arguments that give the possibility to reduce the stability effect to a turbulence intensity effect, and particularly at low Wind speeds.

***/ You are right, using only turbulence intensity (TI) is a very strong simplification for stability. To come up to the readers expectations we will add more clarity to the abstract and introduction to make the purpose of the paper more defined.

The idea behind this research is to find a signal that could be used to improve wake model tuning for specific operational conditions. This may help to improve the use of a wake model to detect underperformance as proposed in Mittelmeier et al. (2017). We will show, that the magnitude of wake effect is not only governed by stability but also turbulence intensity and we will show to which extend one can expect an overlapping effect.
For this purpose, we will provide peer reviewed journal publications to base the assumptions on a more solid foundation and evaluate new data to be able to compare a stability description defined by the Monin-Obukhov similarity theory and the SCADA data.

In Hansen et al. (2012), the authors studied wake effects at Horns Rev in different atmospheric conditions. They also compared turbulence intensities for different stability classes as a function of the wind speed. Below 7m/s a clear increase in TI can be noticed. Above 7m/s neutral-unstable conditions are clearly distinguishable from more stable conditions with a constant threshold up to nominal wind speed. Dörenkämper et al. (2014) published their results also at a peer reviewed conference series where they draw the link from stability via shear to turbulence intensity motivated by the studies of (Tambke et al., 2005). In a later study, Sanz Rodrigo et al. (2015) compared different stability classification methodologies with data from FINO 1 and presented the behavior of shear and turbulence intensity for the proposed atmospheric stability classes. The authors concluded, that in this particular cases TI correlates well for stable cases but at near neutral and unstable cases, shear is supposed to enable better distinction between their nine classes.

We investigated new data from FINO1 to be able to use a “real” stability classification and not only TI classes.
With latest calibrated temperature data from DEWI (Richard Fruehmann) we were able to follow the approach suggested by Ott and Nielsen (2014) and calculated the dimensionless $\zeta = \frac{z}{L}$ for T_air at 33m. The plot below shows the data availability for the selected period.

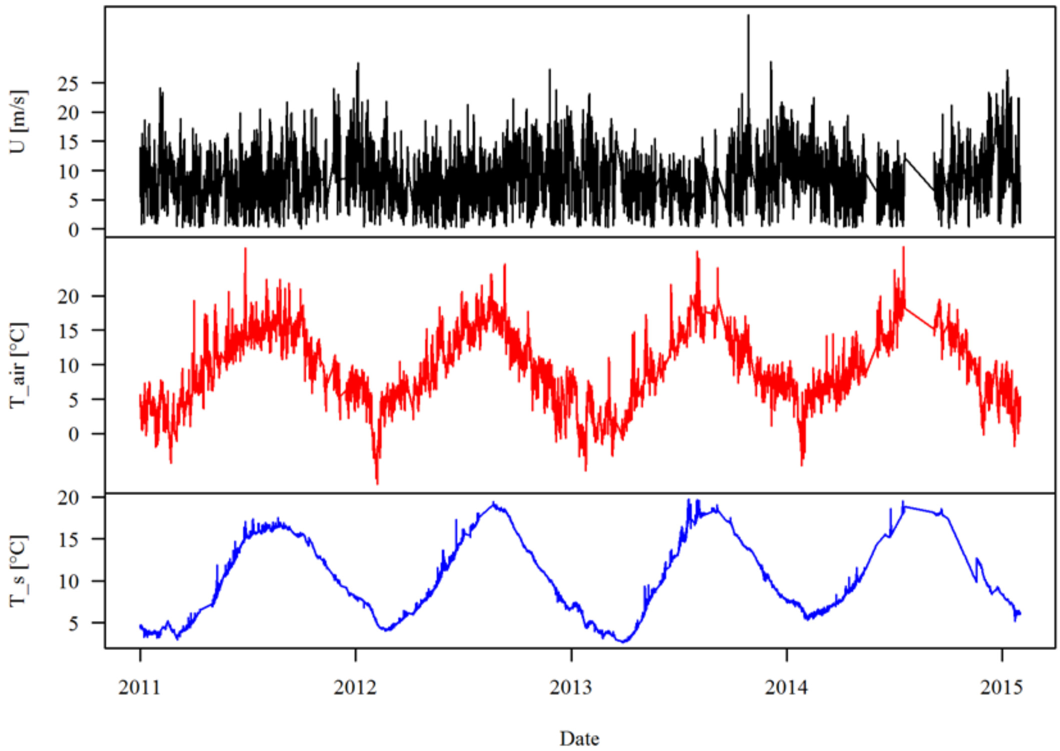

We decided to keep the number of classes at three (“unstable”, “neutral” and “stable”) based on the following table:

Category	Range
Unstable	$\zeta < -0.05$
Neutral	$-0.05 \leq \zeta \leq 0.05$
Stable	$\zeta > 0.05$

(We will add more description of the methodology for the estimation of thresholds in Section 3.3) The estimated thresholds have also been proposed by Rajewski et al. (2013).
This leads to the following histogram for the three classes.

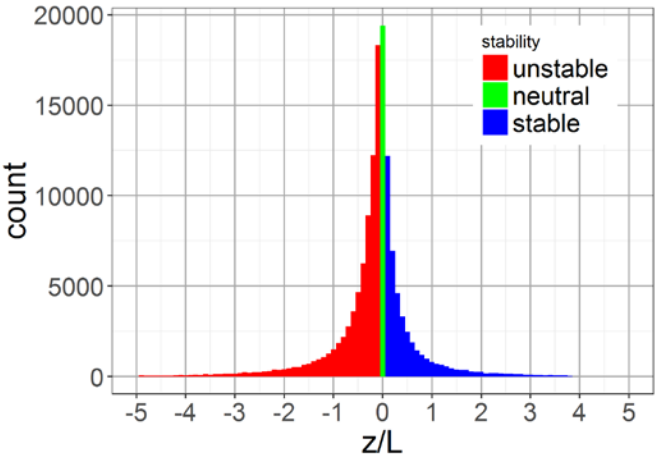

In the plot below, we have used the new stability classification based on $\zeta = z/L$. Bin averaged turbulence intensity (TI_100) measured at the met mast and at the nacelle (AV4_TI) as well as met mast shear (alpha_90_40) and AV4_POTI are plotted for each class as function of the wind speed. The selected wind speed bin of 8 ± 1m/s is quite well distinguishable with constant thresholds for all the provided variables. But whereas turbulence intensity from the met mast is fairly constant for the whole presented range, shear and POTI are showing a much stronger dependency on wind speed.

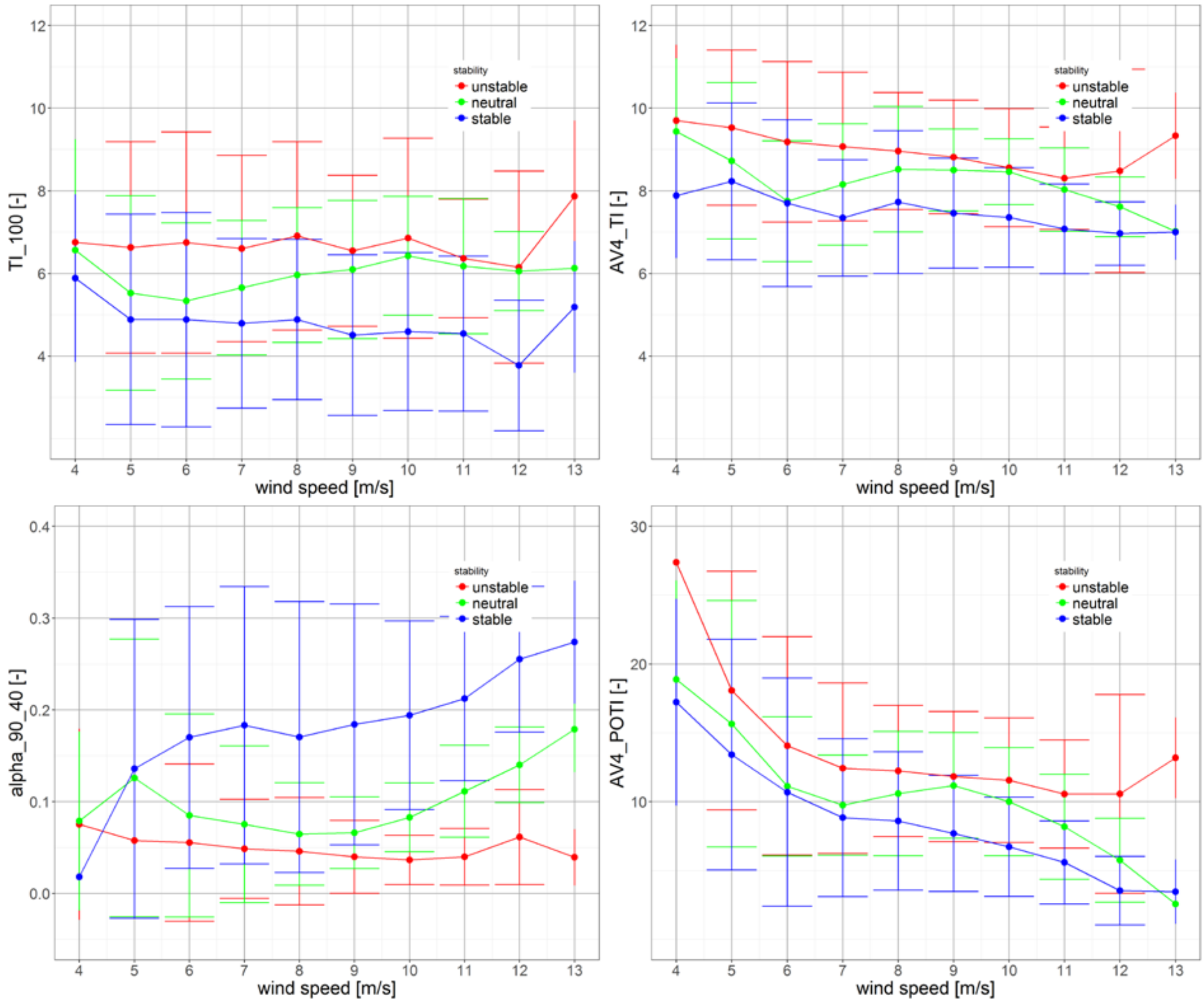

The plots above confirm the statement made by Tambke et al. (2005) and Sanz Rodrigo et al. (2015), that shear enables a more clear distinction between the atmospheric stability classes. The error bars, indicating one standard deviation are not overlapping anymore for stable and unstable class above 8 m/s.

As you have suggested, we will develop the arguments in a new way. We describe how to classify low and high wake effects and use this characteristic to evaluate the predictability based on stability, turbulence intensity and turbine SCADA data classes. Then we provide an overview on the different occurrences of the described environmental conditions.

Determination of thresholds:
At first we select the normalized power (waked turbine, normalized by the power of a free flow turbine) for a small sector (10°) in the full wake for the relevant wind speed range (8 ± 1 m/s) (Fig 1a). Secondly we eliminate the dependency on wind direction by normalizing the normalized power for each wind direction bin (binwidth = 2°) with its mean value (Fig. 1b).

Fig. 1a

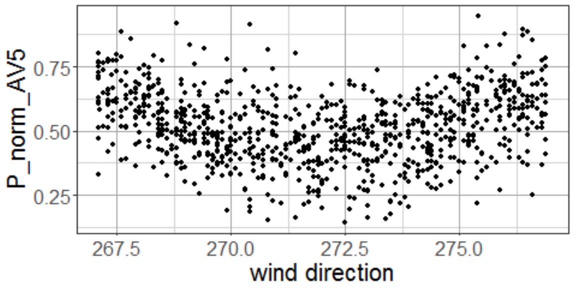

Fig. 1b

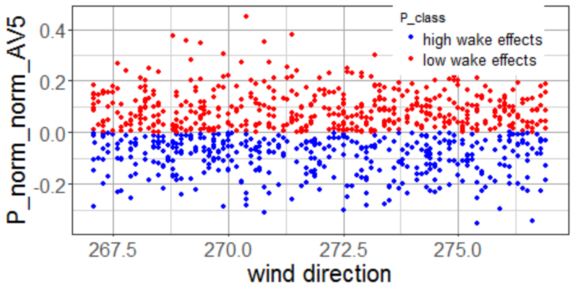

The third step divides the data set into high wake effects (values < 0) and low wake effects (values >= 0) and the density distribution of the variable of interest is plotted for these two data sets (Fig 2). We use the median for each density distribution to allocate thresholds.

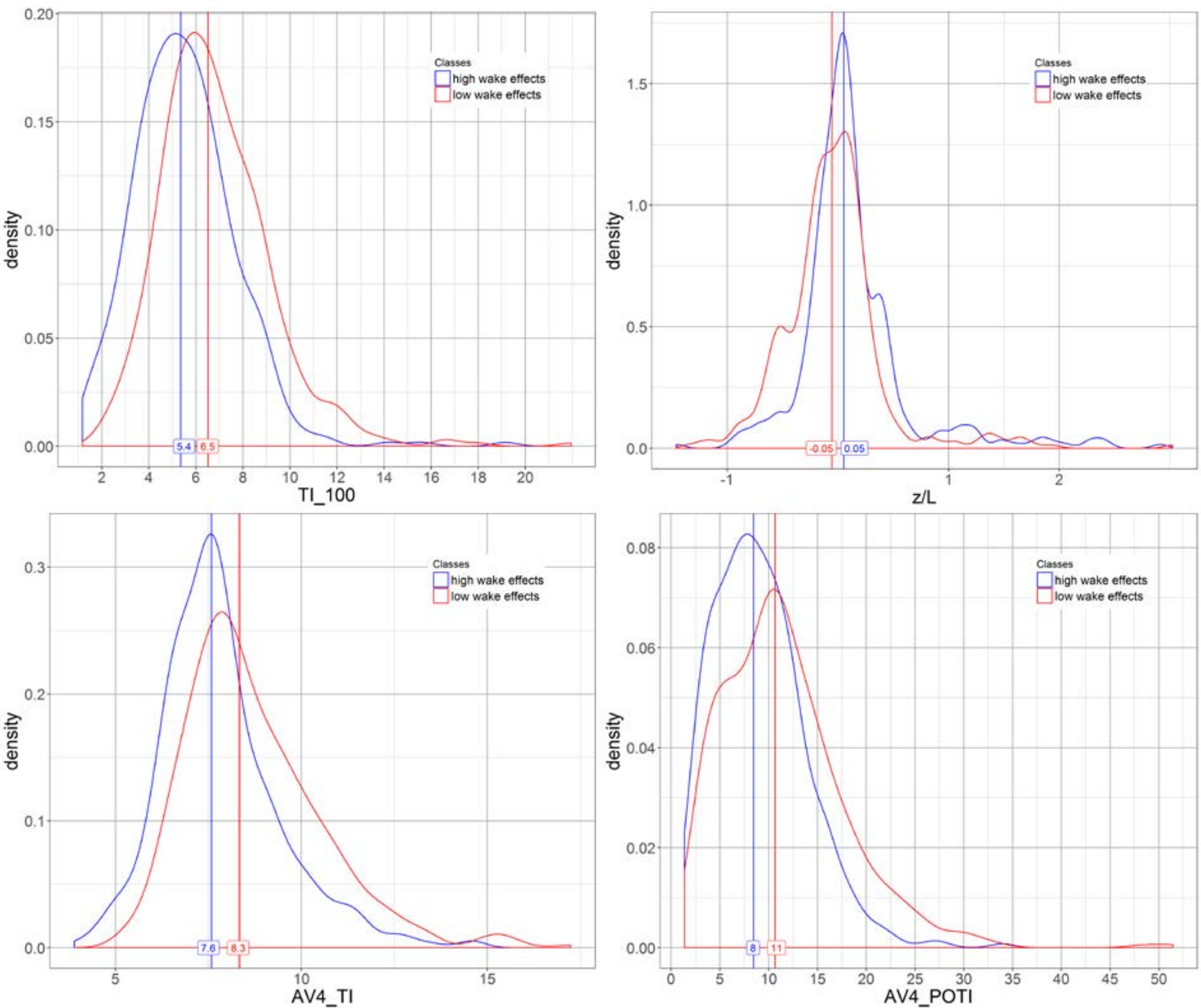

Fig 2. Data density for different variables based on low and high wake effects. The median for each distribution is highlighted with a vertical line. The data corresponds to a wind speed bin of 8 ± 1 m/s and a sector width of 10° around the full wake.

Note:
The TI and POTI thresholds have slightly changed compared to our first version of the paper. The difference in TI thresholds is due to the fact, that we have used the values from Dörenkämper (2015) and now we are suggesting this new methodology.
POTI thresholds have also slightly changed from the old version of our paper because the criteria was visual inspected and now we propose to use the median. In this way, the results should be reproducible now.

To overcome the shortfall of AV4_POTI signal having a strong dependency on wind speed, we propose a normalization of this signal with a third order polynomial.

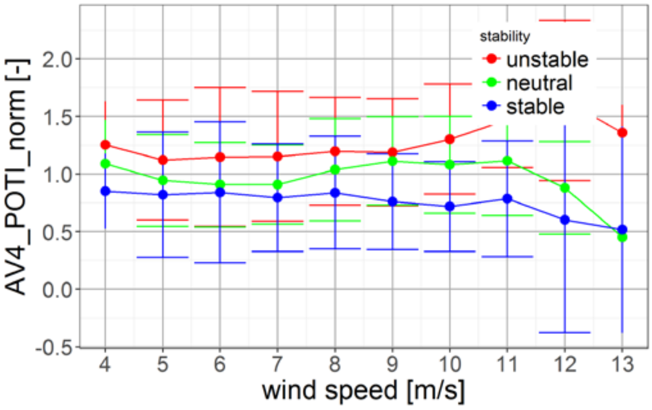

When applying the same methodology to AV4_POTI_norm as described above, we obtain density distributions as below:

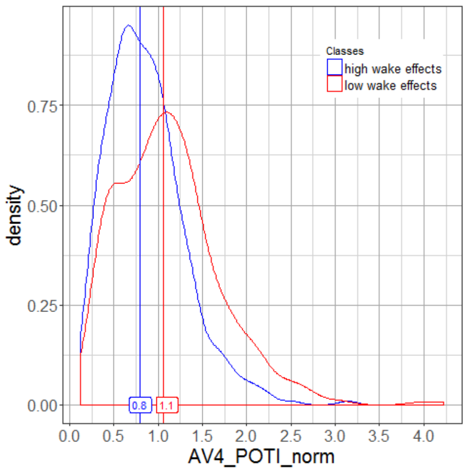

The table below summarizes the different classes:

Category	$\zeta = z/L$ **[-]**	**TI_100 [%]**	**AV4_POTI_norm [-]**
Weak wakes	$\zeta < -0.05$	TI_100 $< 5.4\%$	$POTI_{norm} < 0.8$
Medium wakes	$-0.05 \leq \zeta \leq 0.05$	$5.4 \leq T_{100} \leq 6.5$	$0.8 \leq POTI_{norm} \leq 1.1$
Strong wakes	$\zeta > 0.05$	$T_{100} > 6.5$	$POTI_{norm} > 1.1$

Looking at the distributions for each class, one can see an improvement from POTI to POTI_norm. Latter is much more comparable to the turbulence intensity measured at the met mast.

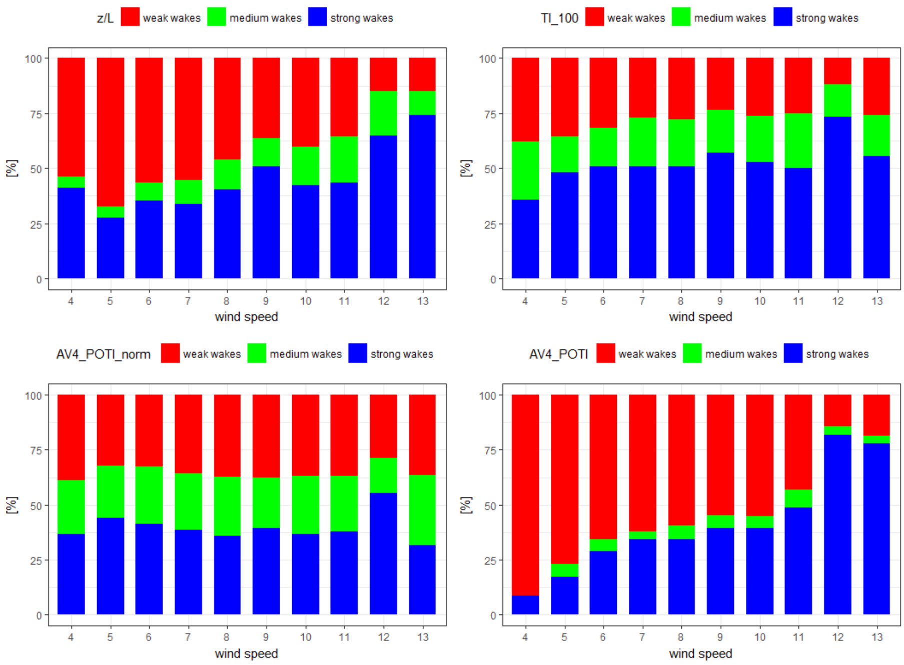

For z/L, weak wakes cases seem to become less frequent with increasing wind speed. POTI seams to overestimate this trend. TI_100 and AV4_POTI_norm provide similar results. Using AV_POTI_norm as a classifier, we obtain the following wake plot:

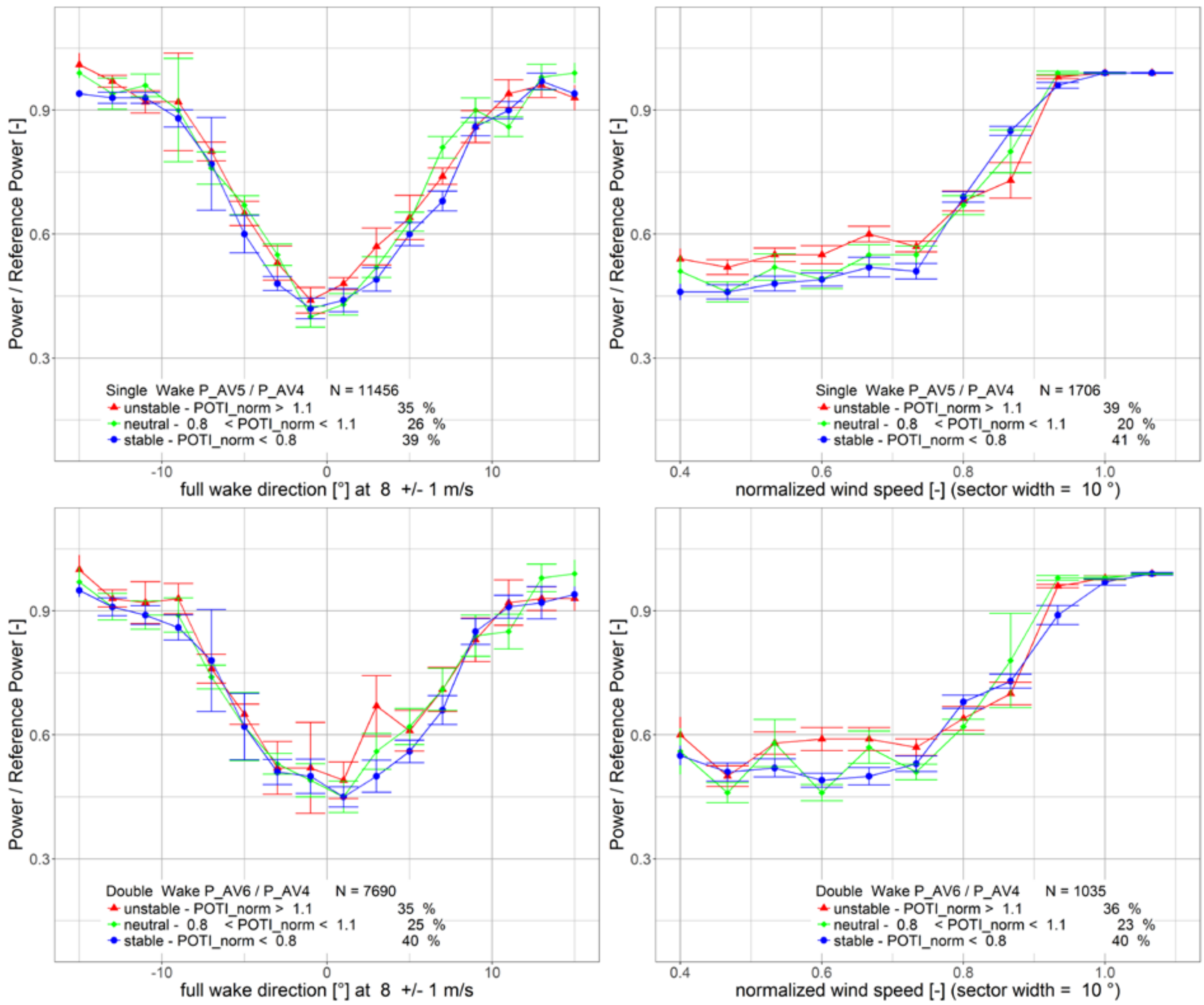

References:
Dörenkämper, M., Tambke, J., Steinfeld, G., Heinemann, D. and Kühn, M.: Atmospheric Impacts on Power Curves of Multi-Megawatt Offshore Wind Turbines, J. Phys. Conf. Ser., 555(1), 12029, doi:10.1088/1742-6596/555/1/012029, 2014.

Mittelmeier, N., Blodau, T. and Kühn, M.: Monitoring offshore wind farm power performance with SCADA data and an advanced wake model, Wind Energy Sci., 2, 175–187, doi:10.5194/wes-2-175-2017, 2017.

Hansen, K. S., Barthelmie, R. J., Jensen, L. E. and Sommer, A.: The impact of turbulence intensity and atmospheric stability on power deficits due to wind turbine wakes at Horns Rev wind farm, Wind Energy, 15(1), 183–196, doi:10.1002/we.512, 2012.

Rajewski, D. A., Takle, E. S., Lundquist, J. K., Oncley, S., Prueger, J. H., Horst, T. W., Rhodes, M. E., Pfeiffer, R., Hatfield, J. L., Spoth, K. K., Doorenbos, R. K., Rajewski, D. A., Takle, E. S., Lundquist, J. K., Oncley, S., Prueger, J. H., Horst, T. W., Rhodes, M. E., Pfeiffer, R., Hatfield, J. L., Spoth, K. K. and Doorenbos, R. K.: Crop Wind Energy Experiment (CWEX): Observations of Surface-Layer, Boundary Layer, and Mesoscale Interactions with a Wind Farm, Bull. Am. Meteorol. Soc., 94(5), 655–672, doi:10.1175/BAMS-D-11-00240.1, 2013.

Sanz Rodrigo, J., Cantero, E., García, B., Borbón, F., Irigoyen, U., Lozano, S., Fernande, P. M., Chávez, R. a, Rodrigo, J. S., Cantero, E., García, B., Borbón, F., Irigoyen, U., Lozano, S., Fernande, P. M. and Chávez, R. a: Atmospheric stability assessment for the characterization of offshore wind conditions, J. Phys. Conf. Ser., 625, 12044, doi:10.1088/1742-6596/625/1/012044, 2015.

Ott, S. and Nielsen, M.: Developments of the offshore wind turbine wake model Fuga, E-0046 Report 2014, DTU Wind Energy, Lyngby, Denmark., 2014.

Tambke, J., Claveri, L., Bye, J. A. T., Poppinga, C., Lange, B., Bremen, L. Von and Wolff, J.: Marine Meteorology for Multi-Mega-Watt Turbines, 2005.

/***

- LiDAR measurements at Nord See wind farm NO : PPI planes are described as horizontal. LiDAR is located on the helicopter platform from the wind turbine NO48. One therefore guess that is corresponds to an altitude close to the hub height. Consequently, the laser beam should meet the wind turbine rotors NO44 and NO45, leading to unusable data in the vicinity of both rotors. On the other hand, on Figure 4, the visualizations of the velocity field, as well as the normalized velocity evolution versus the downwind distance do not present any unresolved areas close to the rotors. The velocity induction through the rotor is presented and discussed. Please explain how these data were reconstructed close to the rotors.

***/ Yes, you are right. Hard targets like blades and nacelle prevent a reasonable wind speed measurement. Due to the fact, that we are using multiple PPI-scans to obtain a 10-min average value, there are wind speed measurements available in the rotor plane.
To derive the wind speeds for Fig. 4 (top), a raster layer was generated. While raster cells with multiple measurements are averaged, values with empty cells are linearly interpolated. In this way, the blind region at each nacelle and areas between the beam directions show interpolated wind speeds.

We will add the following text:
“Hard targets like blades and nacelle prevent reasonable wind speed measurement. Wind speeds at these blind regions and between the beam directions are linearly interpolated. “
/***

- §3.3 New classification and validation. This part is confusing. The authors determine a classification of the wake effect on the basis of the median of the normalized power of a wind turbine in wake interaction. It means that the intensity of the wake effect is determined by its statistical occurrence and not by its strength. Please elaborate an argumentation to justify this strategy of classification

***/ You are right, this part has been not sufficiently described. In our data example we obtained a mean = 0.516 and a median = 0.5108 which is very close together (0.0052). We decided to use the median because the mean was effected by some outliers. A deeper analysis of these outliers revealed that an additional filter criteria for the data is needed. The new filter removes 10-min intervals when one of the turbines has had a downtime in the interval before. In this way the flow throw the wind farm gets another 10-min time to develop. Additionally data with a power ratio > 1 meaning that the turbine in the wake produces more than a free flow turbine has been deleted (only two values). After removing these outliers, mean and median have now a difference of 0.0015. We agree that it is more appropriate to use the mean when enough care for outliers has been taken.

We will describe the new filtering in 2.4 and change 3.3 to "mean" instead of median.
/***

- §4.2 Correlation analysis. It is not clear whether the data are sorted only according to the turbulence intensity or also to the wind speed (as performed in Fig. 5). If the data are not sorted according to the wind speed, it means that different operating conditions are plotted without distinction in this correlation matrix. How can one expect to get strong correlations between data coming from the incoming flow conditions (fully independent of the operation parameters) and operation-driven data coming from the wind turbines without any additional filters ? Could you please show the evolution of the relative power fluctuation PO_TI with the WT power or with the wind speed? Regardless of this crucial point, one cannot state that the level of correlation is acceptable in order to use this information as a representation of the turbulence intensity, and even less of the atmospheric stability.

***/ You are right. Please find below the requested plots. Within the wind speed range of interest, the turbine signal is much more dependent on wind speed than the measured turbulence intensity at the met mast. All our wake plots are based on the wind speed bin 8 ± 1 m/s. In this range the correlation is higher, than for the other wind speeds.

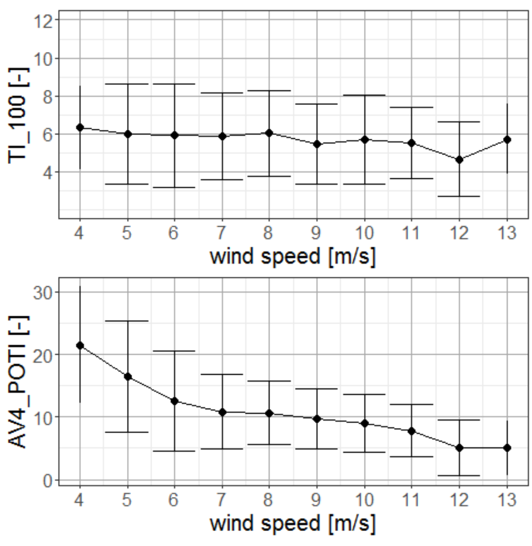

/***

- §4.3.1 New classification and validation on Alpha Ventus. By applying the new classification; discrepancies in the power production due to the assessed stability is rather small and difficult to interpret. By comparing Fig 5 and Fig 9, one notice that the frequency of occurrence of each stability class is also totally dependent of the classification method. For instance, on the top-right plot, the unstable case occurrence is 13% of samples for the new classification, instead of 56% with the classification based on turbulence intensity. It show again the poor correlation between both information.

***/ In Fig. 9 the % values are biased because the "stable" class also contains all data where the turbine controller has already started with the main pitch activity which leads to a lower standard deviation of the power. We have to filter this part of the operation before displaying the proportions of the classes. We will call this part of the data "unclassified". The corrected plot is provided below:

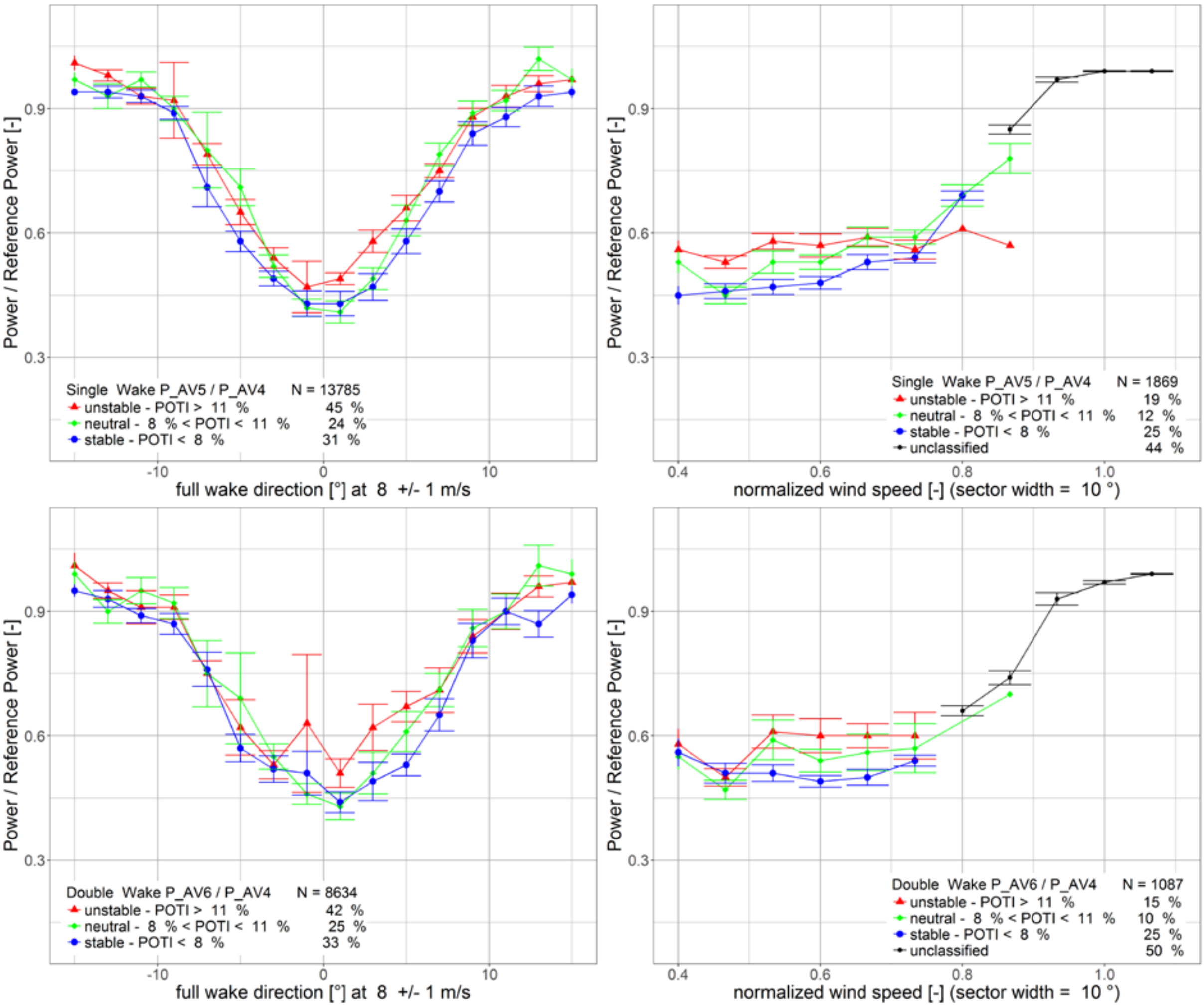

We think this plot is not relevant anymore. We would like to show the new classification based on the normalized AV4_POTI_norm. (As provided for the answer of your first comment)
/***

- The thresholds used in the new classification are different for each tested wind farms. It is justified by the fact that the wind turbines are different. But how can one explain that thresholds are different on the same wind farm (Ormonde) but for different wind directions?

/We assume that this has been an error due to the fact that POTI was very much dependent on wind speed. With the new proposed method to use a normalized values we can stick to the same classification even for different turbines, cause the turbine behavior is canceled out. /

Wind Energ. Sci. Discuss., doi:10.5194/wes-2016-60-RC2, 2017

Interactive comment on

“An analysis of offshore wind farm SCADA measurements to identify key parameters influencing the magnitude of wake effects” by Niko Mittelmeier et al.

Answers to comments from anonymous Referee #2 by

Niko Mittelmeier et al. April 25, 2017

Dear Referee,
Thank you very much for reviewing our paper. Your comments helped us to understand where certainly more explanations is needed and we hope that we could add clarity and additional content to answer your questions sufficiently. You are right, when you point out, that it’s a big step from SCADA data to stability classification and that strong simplifications have been made. For this reason we have accessed more data to close the gap between meteorological stability classification, TI, Shear and SCADA signals. We also want to be more precise on the purpose of this work. The main aim is to find turbine signals which can describe the magnitude of wake effects that are varying with different environmental conditions. With these signals it should be possible to fine tune wake models for more accurate predictions.
Our responses to your comments are marked as ***/ Response /***.

This paper presents a new parameterization of stability classes for the prediction of single and multiple wake effects based on met mast and LiDAR data. After reviewing the paper, I am fairly convinced that this line of reasoning is worth pursuing. However, there are some issues to be addressed before the paper can be recommended for publication. These are enumerated below.

Specific comments

Page 2, line 12 ‘rotordiameter’ is missing a space.

/ changed to “rotor diameter” /

Page 3, fig 2 caption ‘cycles’ should be ‘circles’.

/ changed to “circles” /

Page 4, lines 11 and 12 There are two instances where ‘is’ should be ‘are’.

/both instances changed to “are” /

Page 4, lines 17 and 18 There are two spelling errors: ‘allowes’ and ‘includs’. Also the possessive is not necessary for ‘turbine’ and ‘nacelle’.

/ Changed to “allows” and “includes” and possessives deleted/

Page 6, section 3.1 It is surprising that a study specifically considering stability effects is relying on a simplified classification technique. This introduces a considerable amount of unnecessary uncertainty as an independent variable (i.e. the stability) is not directly measured.

***/ You are right. An acceptable representation of stability is needed and therefore we have accessed new data that has been just recently published on the BSH Fino Server. We will also develop our arguments slightly different. A new reproducible classification (see your comment from page 8) based on the magnitude of wake effects will be used and predictability with the different measured signals ($\zeta = z/L$, turbulence intensity and Turbine SCADA) is studied.

With latest calibrated temperature data from DEWI (Richard Fruehmann) we were able to follow the approach suggested by Ott and Nielsen (2014) and calculated the dimensionless $\zeta = \frac{z}{L}$ for T_air at 33m. The plot below shows the data availability for the selected period.

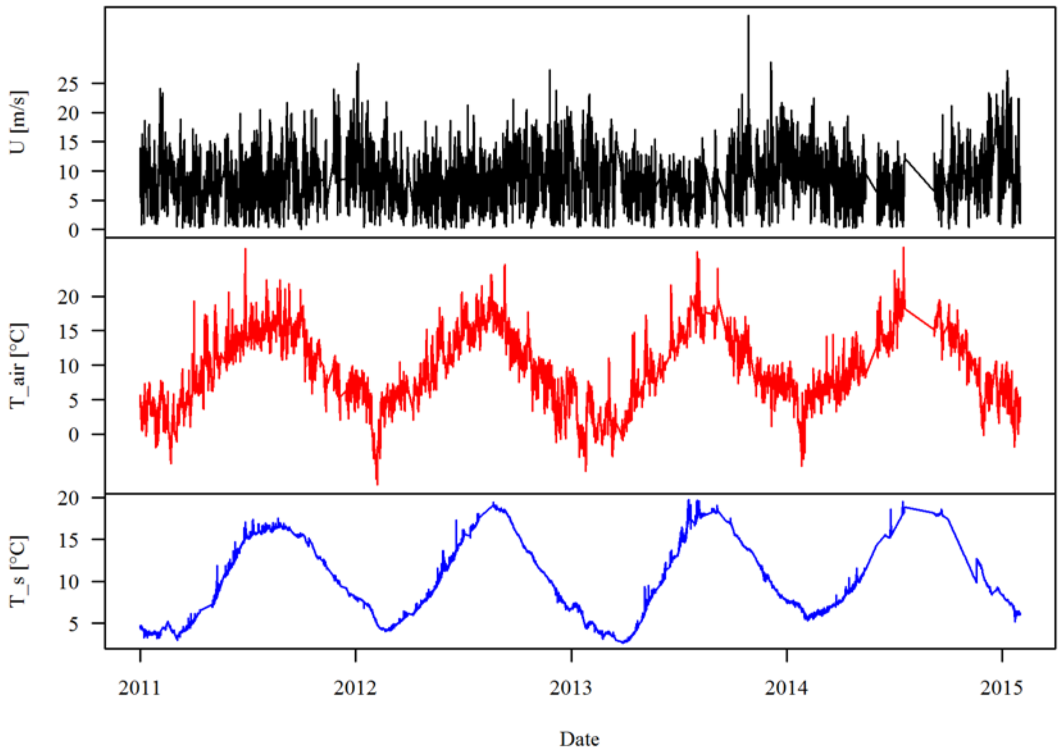

We decided to keep the number of classes at three (“unstable”, “neutral” and “stable”) based on the following table: (We will add more description of the methodology for the estimation of thresholds in Section 3.3, see also your comment for page 8) The estimated thresholds have also been proposed by Rajewski et al. (2013).

Category	Range
Unstable	$\zeta < -0.05$
Neutral	$-0.05 \leq \zeta \leq 0.05$
Stable	$\zeta > 0.05$

This leads to the following histogram for the three classes.

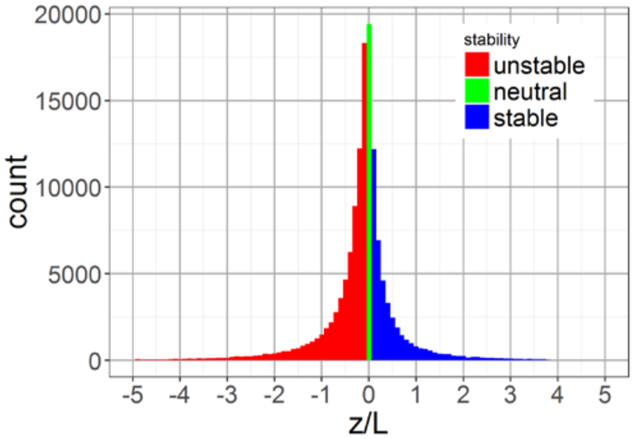

References:

Ott, S. and Nielsen, M.: Developments of the offshore wind turbine wake model Fuga, E-0046 Report 2014, DTU Wind Energy, Lyngby, Denmark., 2014.

Rajewski, D. A., Takle, E. S., Lundquist, J. K., Oncley, S., Prueger, J. H., Horst, T. W., Rhodes, M. E., Pfeiffer, R., Hatfield, J. L., Spoth, K. K., Doorenbos, R. K., Rajewski, D. A., Takle, E. S., Lundquist, J. K., Oncley, S., Prueger, J. H., Horst, T. W., Rhodes, M. E., Pfeiffer, R., Hatfield, J. L., Spoth, K. K. and Doorenbos, R. K.: Crop Wind Energy Experiment (CWEX): Observations of Surface-Layer, Boundary Layer, and Mesoscale Interactions with a Wind Farm, Bull. Am. Meteorol. Soc., 94(5), 655–672, doi:10.1175/BAMS-D-11-00240.1, 2013.

/***

Page 7, table 1 More discussion for the boundary values for TI is needed. How exactly were these values assigned to unstable, neutral, and stable?

***/ The presented values are taken from Dörenkämper (2015). There is no description how exactly these values have been selected. In earlier studies (Dörenkämper et al., 2012, 2014) the authors used 1min averaged data and therefore also different thresholds than in his 2015 studies.
With your later comment, requesting a more solid method to reproduce the assessment of the thresholds we will use our new classification method (See Comment for Page 8) .

References:
Dörenkämper, M., Tambke, J., Steinfeld, G., Heinemann, D. and Kühn, M.: Influence of marine boundary layer characteristics on power curves of multi megawatt offshore wind turbines, in Proceedings of 11th German Wind Energy Conference, Bremen, Germany, 7-8 November., 2012.

Dörenkämper, M., Tambke, J., Steinfeld, G., Heinemann, D. and Kühn, M.: Atmospheric Impacts on Power Curves of Multi-Megawatt Offshore Wind Turbines, J. Phys. Conf. Ser., 555(1), 12029, doi:10.1088/1742-6596/555/1/012029, 2014.

Dörenkämper, M.: An investigation of the atmospheric influence on spatial and temporal power fluctuations in offshore wind farms, PhD Thesis, University of Oldenburg, Oldenburg., 2015.
/***

Page 7, eq 4 I suspect, but cannot verify, that the decent correlation between the two may be (in part) happenstance. Atmospheric turbulence intensity decreases with wind speed as a result of flow physics. The standard deviation of output power to power also decreases with wind speed but largely because the turbine controller plays an increasingly active role. The authors allude to this later in the paper but more discussion of why eq 4 might be a suitable proxy for eq 1 would be of interest.

***/ This is a very valid point. Therefore we have investigated more on the influence of wind speed. In the plot below, we have used the new stability classification based on $\zeta = z/L$ (See comment for Page 6). Bin averaged turbulence intensity (TI_100) measured at the met mast and at the nacelle (AV4_TI) as well as met mast shear (alpha_90_40) and AV4_POTI are plotted for each class as function of the wind speed. The selected bin of 8 ± 1m/s is quite well distinguishable with constant thresholds for all the provided variables. Whereas turbulence intensity from the met mast is fairly constant for the selected wind speed range, shear and POTI are showing a strong dependency on wind speed.

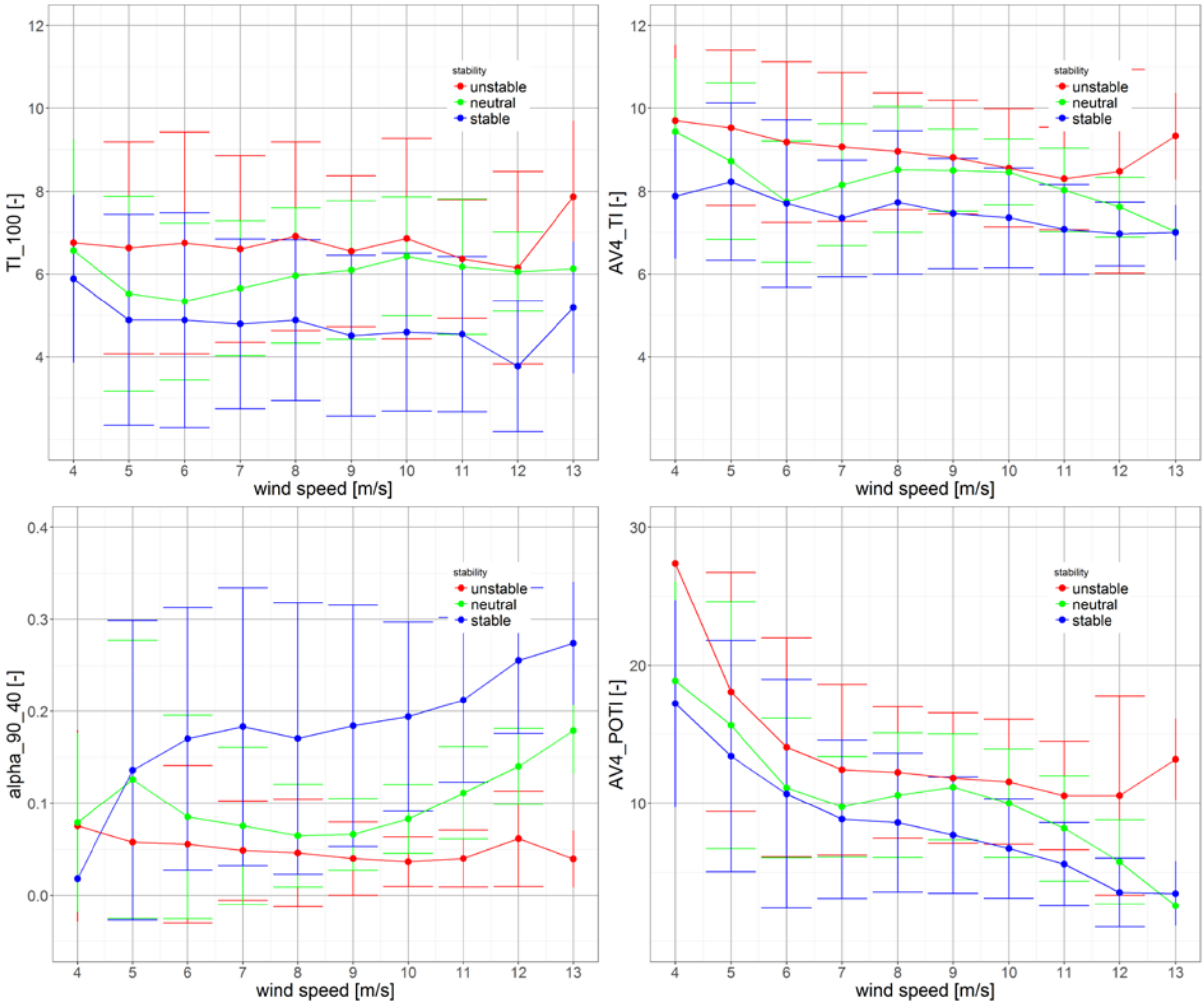

For this reason we propose to develop Eq. 5 which takes wind speed measured at the nacelle also into account.

We are now proposing a correction for POTI to substitute the wind speed dependency. This can be done by normalizing POTI with a third order polynomial. The resulting plot is shown below.

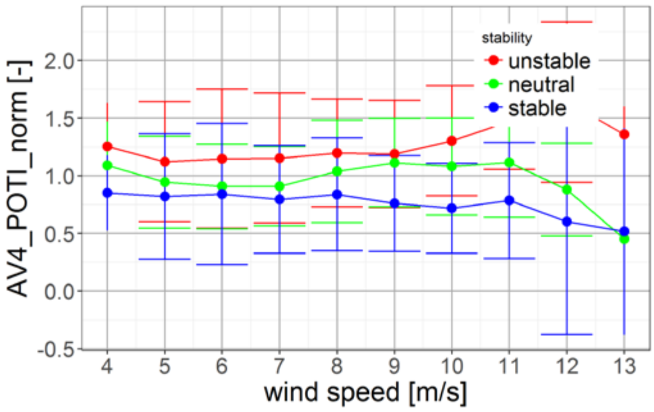

/***

Page 7, line 26 Why use the median instead of the mean?

***/ In our data example we obtained a mean = 0.516 and a median = 0.5108 which is very close together (0.0052). We decided to use the median because the mean was effected by some outliers. A deeper analysis of these outliers revealed that an additional filter criteria for the data is needed. The new filter removes 10-min intervals when one of the turbines has had a downtime in the interval before. In this way the flow throw the wind farm gets another 10-min time to develop. Additionally data with a power ratio > 1 meaning that the turbine in the wake center (±5°) produces more than a free flow turbine has been deleted (only two values). After removing these outliers, mean and median have now a difference of 0.0015. We agree that it is more appropriate to use the mean when enough care for outliers has been taken.

We will describe the new filtering in 2.4 and change 3.3 to "mean" instead of median.
/***

Page 8, line 2 '...the thresholds are selected to achieve the best distinction between the three data sets.' As these thresholds are central to the stability classification (and this work in general), a mathematical definition of best distinction must be included. Currently, this work is unreproducible by a third party.

***/ This is a very valid point. We will describe the methodology in more detail:

At first we select the normalized power (waked turbine, normalized by the power of a free flow turbine) for a small sector (10°) in the full wake for the relevant wind speed range (8 ± 1 m/s) (Fig 1a). Secondly we eliminate the dependency on wind direction by normalizing the normalized power for each wind direction bin (binwidth = 2°) with its mean value (Fig. 1b).

Fig. 1a

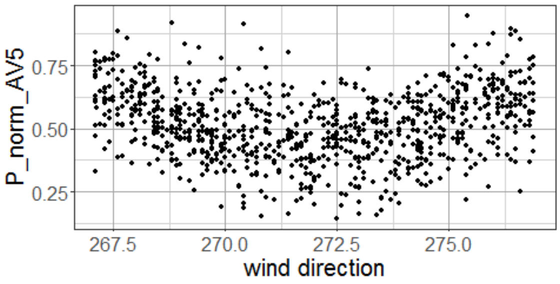

Fig. 1b

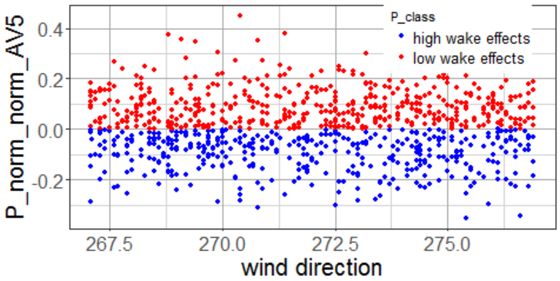

The third step divides the data set into high wake effects (values < 0) and low wake effects (values >= 0) and the density distribution of the variable of interest is plotted for these two data sets (Fig 2). We use the median for each density distribution to allocate the thresholds.

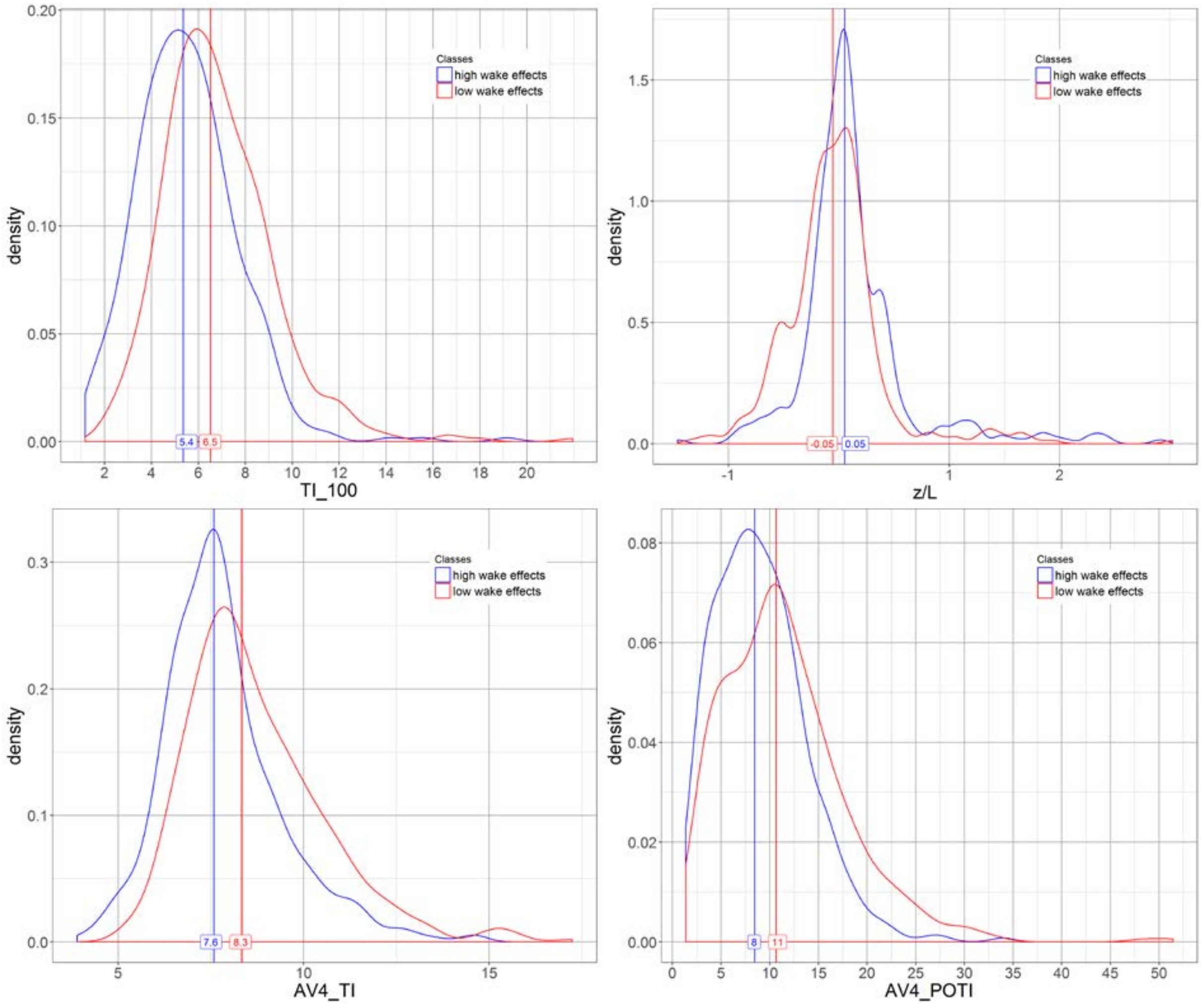

Fig 2. Data density for different variables based on low and high wake effects. The median for each distribution is highlighted with a vertical line. The data corresponds to a wind speed bin of 8 ± 1 m/s and a sector width of 10° around the full wake.

Note:
The TI and POTI thresholds have slightly changed compared to our first version of the paper. The difference in TI thresholds is due to the fact, that we have used the values from Dörenkämper (2015) and now we are suggesting this new methodology.
POTI thresholds have also slightly changed because the criteria was visual inspected and now we propose to use the median. In this way, the results should be reproducible now.

To overcome the shortfall of AV4_POTI signal having a strong dependency on wind speed, we propose a normalization of this signal with a third order polynomial.

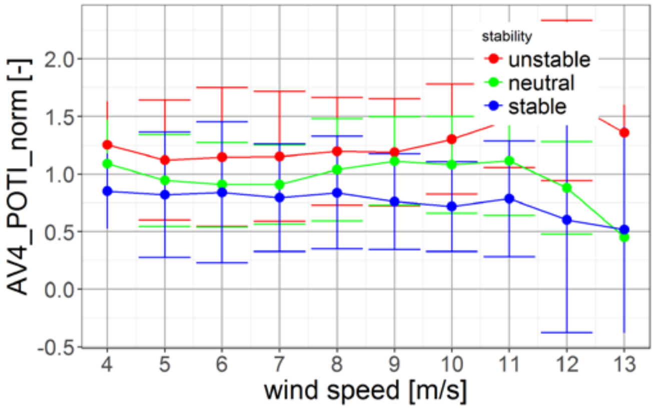

When applying the same methodology to AV4_POTI_norm as described above, we obtain a density distribution as below:

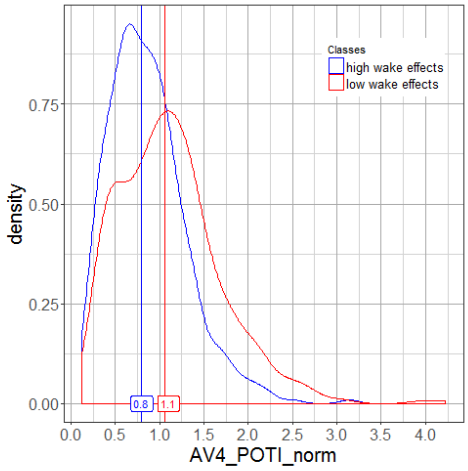

The table below summarizes different classes of interest:

Category	$\zeta = z/L$ [-]	TI_100 [%]	AV4_POTI_norm [-]
Weak wakes	$\zeta < -0.05$	TI_100 $<$ 5.4%	$POTI_{norm} < 0.8$
Medium wakes	$-0.05 \leq \zeta \leq 0.05$	$5.4 \leq T_{100} \leq 6.5$	$0.8 \leq POTI_{norm} \leq 1.1$
Strong wakes	$\zeta > 0.05$	$T_{100} > 6.5$	$POTI_{norm} > 1.1$

Looking at the distributions for each class, one can see an improvement from POTI to POTI_norm. Latter is much more comparable to the turbulence intensity measured at the met mast.
For z/L, weak wakes cases seem to become less frequent with increasing wind speed. POTI seams to overestimate this trend. TI_100 and AV4_POTI_norm provide similar results.

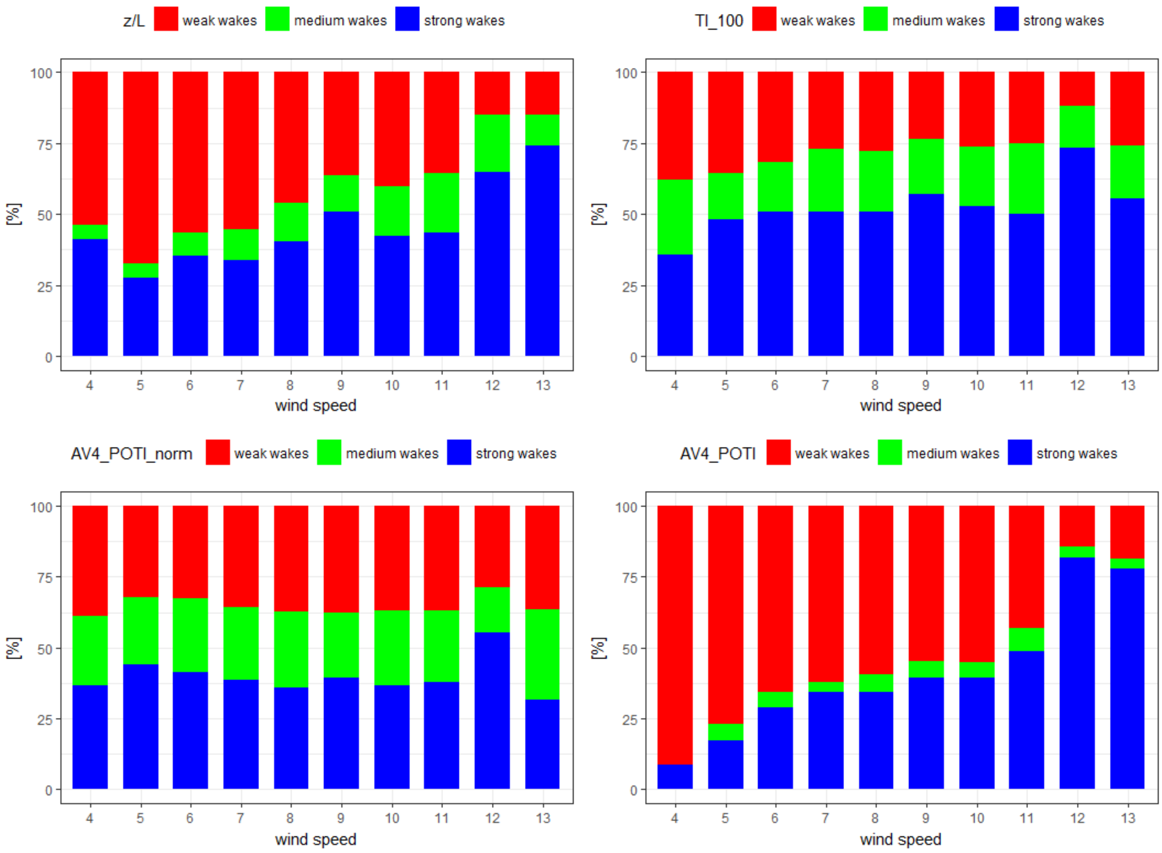

Using AV_POTI_norm as a classifier, we obtain the following wake plot:

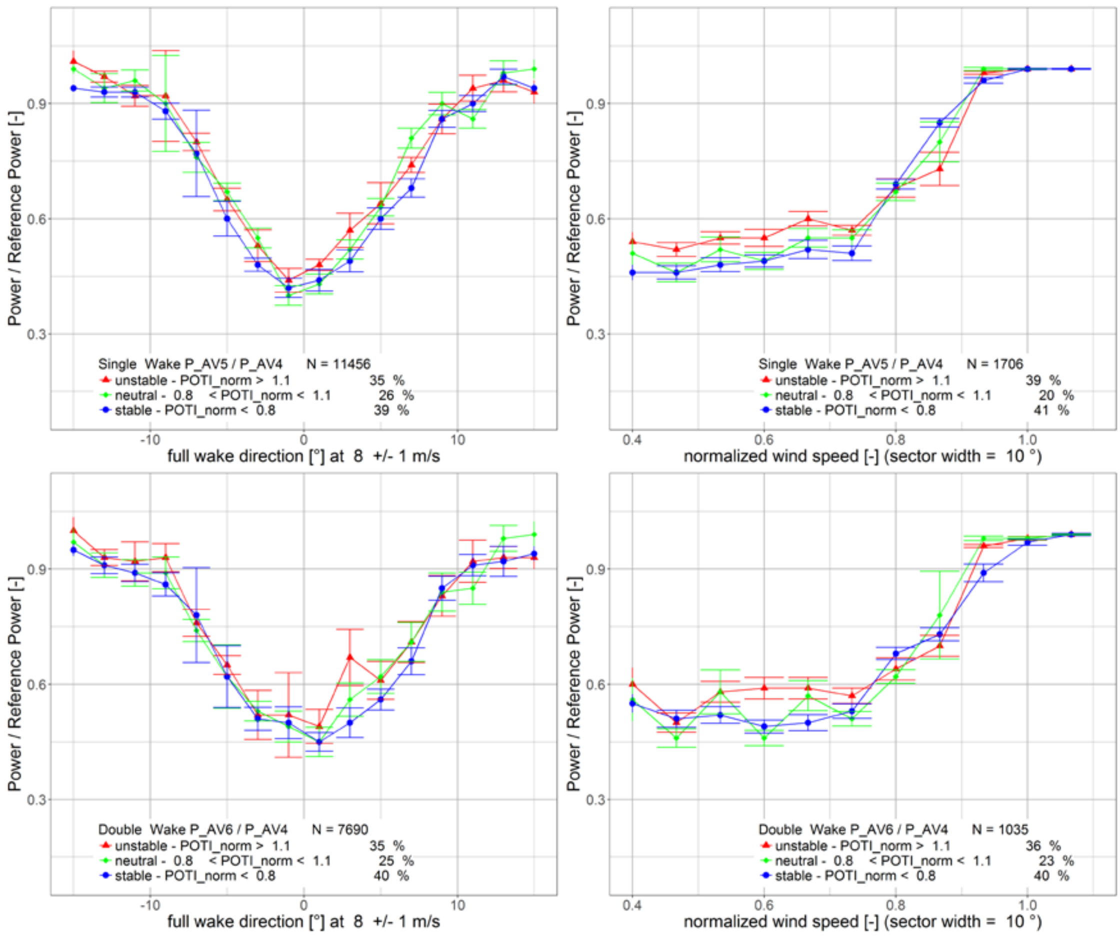

References:

Dörenkämper, M.: An investigation of the atmospheric influence on spatial and temporal power fluctuations in offshore wind farms, PhD Thesis, University of Oldenburg, Oldenburg., 2015.

/***

Page 8, line 7 Please avoid use of the word 'prove' in this context.

/ "prove" replaced by "shows"/

Page 9, fig 5, bottom left One point just right of the centre for the stable curve is clearly an outlier. Any comment? Tables 2–5 The large variation in thresholds suggests that the approach is not general and more details regarding how these thresholds are determined is needed.

***/ We have inspected the outlier and added two new filter criteria. The new filter removes 10-min intervals when one of the turbines has had a downtime in the interval before. In this way the flow throw the wind farm gets another 10-min time to develop. Additionally data with a power ratio > 1 meaning that the turbine in the full wake (wake center ±5°) produces more than a free flow turbine has been removed.

The new plot:

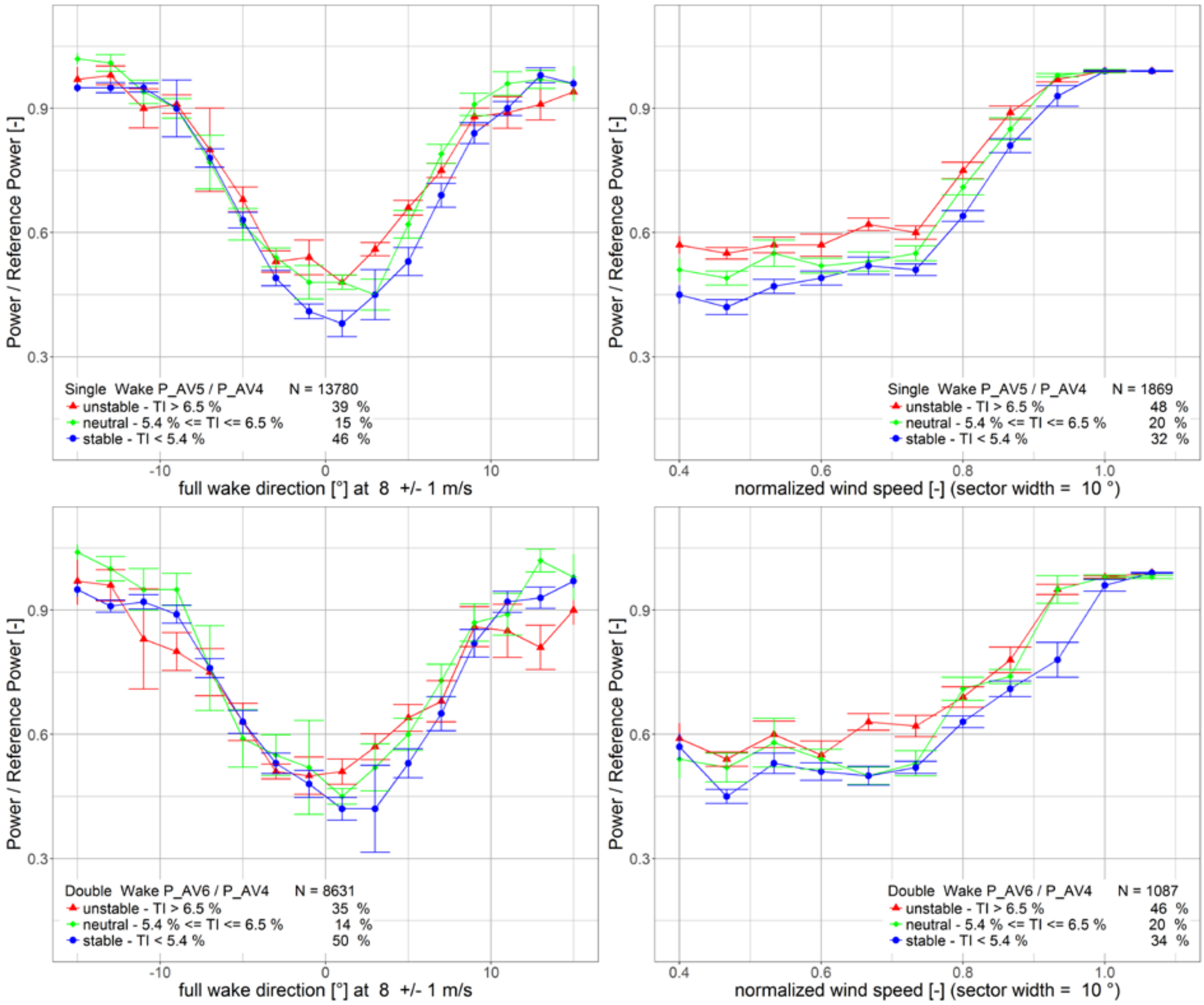

/***

Page 16, line 19 Why limit the data set to 7–9 m/s? Are these results representative?

/We will change the wording from “7-9 m/s” to “8 ± 1 m/s”. In this way it is consistent to the Fig. 5, Fig. 9 and Fig. 13. /

Page 17, line 1 ‘The difference in power production between stable and unstable cases is in the range of 10%.’ Stability is only inferred here from TI so the statement should preferably refer to differences between high and low TI conditions.

***/Agreed!
New wording:
“The difference in power production between high and low turbulence conditions is in the range of 10%, …/***

Page 17, line 8 The paper would be significantly more complete with this range of important wind speeds included in the analysis.

/ That’s true, we are working on it/

Page 18, line 7 Typo: ‘reviled’ should be ‘revealed’.

/changed to “revealed”/